


Origin of high-Cr podiform chromitites from Kabaena Island, Southeast Sulawesi, Indonesia: constraints from mineralogy and geochemistry

Junhua Yao, Jinhong Xu, Chengquan Wu, Zhengwei Zhang, Mega Fatimah Rosana, Xiyao Li & Ziru Jin


To cite this article: Junhua Yao, Jinhong Xu, Chengquan Wu, Zhengwei Zhang, Mega Fatimah Rosana, Xiyao Li & Ziru Jin (2023) Origin of high-Cr podiform chromitites from Kabaena Island, Southeast Sulawesi, Indonesia: constraints from mineralogy and geochemistry, International Geology Review, 65:19, 2943-2960, DOI: [10.1080/00206814.2023.2167130](https://doi.org/10.1080/00206814.2023.2167130)

To link to this article: <https://doi.org/10.1080/00206814.2023.2167130>

 View supplementary material [↗](#)

 Published online: 16 Jan 2023.

 Submit your article to this journal [↗](#)

 Article views: 159

 View related articles [↗](#)

 View Crossmark data [↗](#)

 Citing articles: 1 View citing articles [↗](#)



Origin of high-Cr podiform chromitites from Kabaena Island, Southeast Sulawesi, Indonesia: constraints from mineralogy and geochemistry

Junhua Yao^a, Jinhong Xu^{b,c}, Chengquan Wu^{id}^c, Zhengwei Zhang^c, Mega Fatimah Rosana^d, Xiyao Li^c and Ziru Jin^c

^aCenter of Deep Sea Research & Key Laboratory of Marine Geology and Environment, Institute of Oceanology, Chinese Academy of Sciences, Qingdao, China; ^bSchool of Economics and Management, Tongren University, Guizhou, China; ^cState Key Laboratory of Ore Deposit Geochemistry, Institute of Geochemistry, Chinese Academy of Sciences, Guiyang, China; ^dFaculty of Geology, University of Padjadjaran, Jatinangor, Sumedang, Indonesia

ABSTRACT

The East Sulawesi Ophiolite, one of the three largest ophiolites in the world, contains important podiform chromitites. However, the origin of these chromite deposits is not well constrained. Here, we present the detailed mineralogy and in situ chemistry of chromite and solid inclusions within chromite for podiform chromitites from the Kabaena Island, Southeast Sulawesi. Chromite grains have low TiO₂ (0.17–0.27 wt%) and Al₂O₃ (13.4–15.1 wt%) contents and high Cr# [Cr/(Cr+Al), molar] of 0.70–0.74 and Mg# [Mg/(Mg+Fe²⁺), molar] of 0.69–0.75, which resemble those of other high-Cr podiform chromitites worldwide. The MORB-normalized patterns for some selected major-trace elements of chromite show slightly positive slopes from Al₂O₃ to Mn. Chromite-hosted silicate inclusions include olivine, clinopyroxene, orthopyroxene and amphibole and are characterized by higher Mg/Fe ratios than those of host peridotites. The geothermobarometry of chromite-hosted clinopyroxene-orthopyroxene pairs indicates that the estimated T-P conditions of the parental magma of the Kabaena chromitites are 950–1010°C and 7.0–8.4 Kbar. The extreme-Mg-rich olivine inclusions (Fo >96) with extremely high Ni (5300–8200 ppm) and Cr (1500–6700 ppm) contents are interpreted to have crystallized from high-Mg and Cr boninitic melts, and the Fo contents were then elevated by subsolidus re-equilibration (Fe–Mg and Fe–Ni exchange) with chromite. Sulfide inclusions contain base metal minerals containing millerite with rare pentlandite and chalcopyrite, and platinum-group minerals that include the laurite-erlichmanite series, Ir–Ni monosulfide, irarsite and cuproiridsite. This sulfide assemblage reveals that their parental magmas experienced the evolution of high T and low *f*(S₂) to low T and high *f*(S₂) from the early to late stage. Finally, combined with the palaeogeographic reconstruction in Sulawesi, we propose that the high-Cr chromitites in this region were formed by the reaction of depleted mantle and boninitic magma beneath a juvenile island arc, implying the initiation of a new subduction in the Miocene.

ARTICLE HISTORY

Received 05 October 2022
Accepted 07 January 2023

KEYWORDS

Chromite; Silicate inclusions; PGM; High-Cr chromitites; Sulawesi

1. Introduction

Podiform chromitites, usually with discontinuous, pod-like shapes, are hosted in ophiolitic peridotites and are widely considered to have formed by melt-rock interaction (e.g. Arai and Yurimoto 1994; Zhou *et al.* 1994). These chromitites are usually smaller ore bodies than those from layered intrusions, but they supply more than half of the world's chromite ore production due to the high Cr/Fe or Al/Fe ratios (Stowe 1987). According to the Cr# [Cr/(Cr+Al), molar] of chromite, podiform chromitites can be divided into two types: high-Cr (Cr# >0.6; high Cr/Fe) and high-Al (Cr# <0.6; high Al/Fe) chromitites. The former are thought to be related to boninitic melts and depleted mantle (e.g. harzburgite) that

experienced a high degree of partial melting in fore-arc-related settings (e.g. Pagé and Barnes 2009; Nayak *et al.* 2021; Sideridis *et al.* 2021). The latter are possibly related to MORB-like or arc tholeiite magmas and fertile mantle (e.g. Iherzolite) that experienced a low degree of partial melting in a MORB or back-arc setting (e.g. Zhou *et al.* 1998, 2001; Uysal *et al.* 2009; González-Jiménez *et al.* 2011). The podiform chromitites formed in different tectonic environments could preserve different compositional features in terms of mineralogy and geochemistry. Therefore, the study of the genesis of podiform chromite deposits has important significance in not only exploring new chromium resources but also understanding the tectonic

CONTACT Jinhong Xu ✉ xujinhong2011@126.com; Chengquan Wu ✉ wuchenquan@vip.gyig.ac.cn 📧 State Key Laboratory of Ore Deposit Geochemistry, Institute of Geochemistry, Chinese Academy of Sciences, Guiyang 550081, China

This article has been corrected with minor changes. These changes do not impact the academic content of the article.

📎 Supplemental data for this article can be accessed online at <https://doi.org/10.1080/00206814.2023.2167130>.

© 2023 Informa UK Limited, trading as Taylor & Francis Group

evolution of host ophiolites (e.g. Pagé and Barnes 2009; Akmaz *et al.* 2014; Pujol-Solà *et al.* 2021; Sepidbar *et al.* 2021).

Chromite can be an early crystalline phase from mafic-ultramafic magma (e.g. Yao *et al.* 2018) or a residual phase of mantle peridotites after melt extraction (e.g. Arai 1980; Bao 2009). It is more resistant to alteration and weathering than silicate minerals (e.g. olivine and pyroxene). Chromite usually hosts various individual and/or multiphase mineral inclusions in it (Melcher *et al.* 1997; Zhou *et al.* 2014), such as silicate minerals, base metal sulfides (BMS) and platinum-group minerals (PGM). Hence, chromite grains can effectively preserve information about the chemical composition and formation conditions of the parental magma in equilibrium with them. The structure and chemical composition of chromite as well as chromite-hosted mineral inclusions have been widely used to infer the nature of parental melts, the thermochemical conditions of genesis and the tectonic setting of podiform chromitites and igneous rocks in different environments (e.g. Irvine 1965, 1967; Barnes and Roeder 2001; Kamenetsky *et al.* 2001; Rollinson 2008; González-Jiménez *et al.* 2011; Yao *et al.* 2018, 2019, 2021a; Hu *et al.* 2022).

The East Sulawesi Ophiolite (ESO), Indonesia, which is one of the three largest ophiolites in the world along with the Oman Ophiolite and the Papua New Guinea Ophiolite (Kadarusman *et al.* 2004), contains small podiform chromite deposits (Zaccarini *et al.* 2016; Septiana *et al.* 2021). Previous studies have chiefly focused on the petrogenesis of the ESO. A consensus was initially reached on the ability to trace the ESO back to the proximity of the presently active region of the SW Pacific Superplume based on its geochemical features and palaeogeographic reconstruction (Monnier *et al.* 1995; Parkinson 1998; Kadarusman *et al.* 2004). A few of mineralogical study have been carried out on chromitites hosted in the ESO of Sulawesi, Indonesia (Zaccarini *et al.* 2016; Hasria *et al.* 2021; Septiana *et al.* 2021). The composition of these chromitites showed a variation from high-Al to high-Cr contents. However, to our knowledge, no comprehensive studies on the trace element compositions of chromite and the mineral phases of chromite-hosted solid inclusions in the ESO have been conducted to date. In this study, we present the first trace element data of chromite as well as detailed observations of mineral phases within chromite for podiform chromitites from Kabaena Island, Southeast Sulawesi, Indonesia. These datasets are used to reveal the nature of the parental magma and the formation conditions and tectonic setting for the Kabaena chromitites. Combined with previously reported data of other chromite deposits in the ESO and the reconstructed

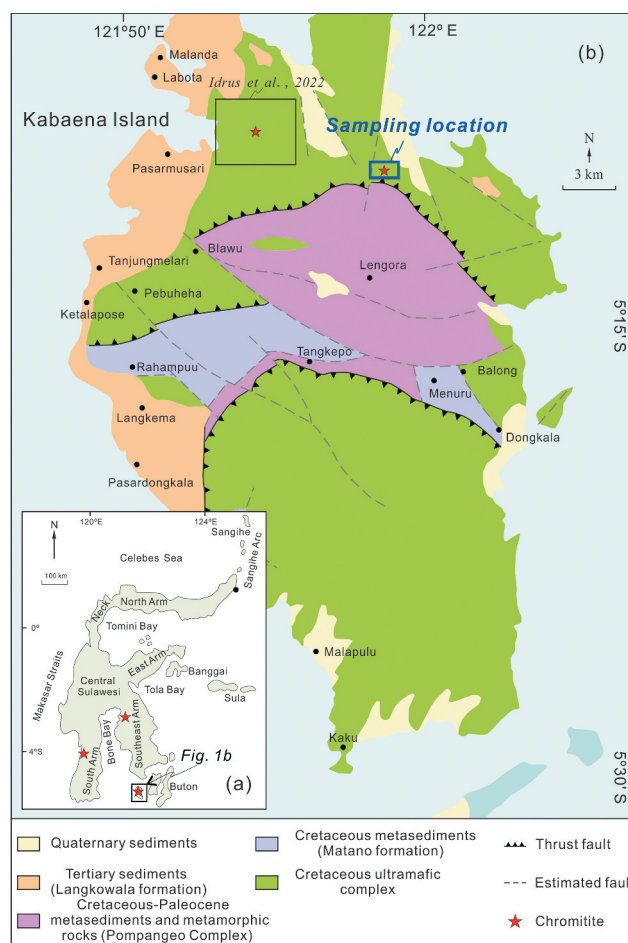


Figure 1. (a) Schematic map showing the tectonic units of Sulawesi Island (modified from Kadarusman *et al.* 2004). (b) Geological map of Kabaena Island, showing the sampling locations (modified from Simandjuntak *et al.* 1993).

palaeogeography of the ESO, we propose a genetic model for the Sulawesi chromitites and provide new constraints on the tectonic evolution in this region.

2. Geological background and sample description

The K-shaped island of Sulawesi (Figure 1a), located in the triple junctions between the Eurasian, Indo-Australian and Pacific mega-plates, is a complex tectonic zone with large-scale tectonic dislocations and thrust faults (e.g. Katili 1978; Parkinson 1996; Hall and Wilson 2000). It is mainly composed of four geological provinces: (1) the West and North Sulawesi volcano-plutonic arc with Cenozoic volcanic and plutonic rocks; (2) the Central Sulawesi metamorphic belt with high-pressure metamorphic rocks, such as Pompangeo schists and an ophiolite mélangé; (3) the East Sulawesi Ophiolite; and (4) two Australian microcontinental fragments, Banggai Sula and Tukang Besi. The East Sulawesi

Ophiolite, with an outcrop area of 15,000 km², is widely distributed from Gorontalo Bay through the East Arm and central Sulawesi towards the Southeast Arm and the islands of Buton and Kabaena (Silver *et al.* 1983; Kadarusman *et al.* 2004). The ages of the basalt and gabbro from the ESO range from the Cretaceous (79–137 Ma) to the Neogene (16–23 Ma) (Simandjuntak 1992; Mubroto *et al.* 1994; Monnier *et al.* 1995; Bergman *et al.* 1996; Parkinson 1998). The ESO contains the full suite of ophiolite lithologies, including residual mantle peridotites, mafic–ultramafic cumulates, layered to isotropic gabbros, sheeted dolerites and basaltic volcanic rocks from bottom to top, and has experienced various degrees of serpentinization in different localities (Parkinson 1998). Numerous chromitites have been found in the Alekale, Bette, Jempulu, Kalamasse, Kamara and Palakka areas from the South Arm, the Latao and Soroako areas from the Southeast Arm, and the Utara and Tedubara areas from Kabaena Island (Zaccarini *et al.* 2016; Hasria *et al.* 2021; Septiana *et al.* 2021; Idrus *et al.* 2022). These deposits are small and irregular pods or nodules hosted in serpentinized peridotites.

Kabaena Island is in the southernmost part of the Southeast Sulawesi Arm. The age of Kabaena Island and the surrounding area varies from the Cretaceous to the Middle Miocene (Hall and Sevastjanova 2012). Due to the division of the South Banda Sea, this island was pushed closer to the Southeast Sulawesi Arm during the Pleistocene (Kadarusman *et al.* 2004; Hall and Sevastjanova 2012). The Pompangeo schist complex consists of Cretaceous and Tertiary low- to moderate-grade metamorphic rocks of phyllite, mica schist, amphibole schist, and chlorite schist (Parkinson 1998). The Matano Formation contains Cretaceous limestone with local metamorphism (Simandjuntak *et al.* 1987; Fadhlurrohman *et al.* 2017). The peridotite unit of the ESO is mainly distributed in the northern and southern portions of the island and primarily consists of lherzolite (Simandjuntak *et al.* 1993). A few harzburgites and dunites can be observed in the northern portion. These ultramafic rock samples from Kabaena Island exhibit some MORB-like geochemical features, such as the MORB-like REE pattern of clinopyroxene (Kadarusman *et al.* 2004). Two large thrust faults with west-east directions across Kabaena Island shifted the ultramafic complex over the Pompangeo schist complex, and the Kabaena metasediments in the Mesozoic (Nursahan 2005). Tertiary and Quaternary sediments cover the ultramafic complex (Figure 1b).

The chromitite samples investigated in this study were collected from field outcrops and local mines in the northern part of the island, where there is relatively dense vegetation and a high hilly morphology (Figure 2a–d). The latitude and longitude of the sampling locations are

listed in Supplementary Table S1. Chromitite orebodies with lens or nodule shapes are hosted in harzburgites and have thicknesses ranging from tens of centimetres to a few metres. The host harzburgites have a typical granular texture and have experienced various degrees of weathering and alteration. The chromite aggregates occur interstitially to grains of olivine and orthopyroxene (Figure 2e–f). As the chromite content increases, the type of mineralization is defined as disseminated, net-textured, and massive. Most of the chromite grains are reddish-brown unaltered crystals that are variable in size (0.5–2 cm) and embedded in an altered silicate matrix. Along the rims and cracks, chromite is replaced by magnetite/ferrian chromite. Olivine in the matrix is generally replaced by serpentine, with a small amount of unaltered residual fragments (Figure 2e–f). Many silicate and sulfide inclusions are detected in unaltered chromite grains from the Kabaena chromitites (Figure S1).

3. Analytical methods

The compositions of solid inclusion mineral and chromite from the Kabaena chromitites and host rocks (harzburgites) were determined using wavelength dispersive analysis with a JEOL JXA-8530 F Plus electron microprobe (EPMA) at the State Key Laboratory of Ore Deposit Geochemistry, Institute of Geochemistry, Chinese Academy of Sciences in Guiyang. The analytical conditions included an accelerating voltage of 25 kV, a beam current of 10 nA, and a peak counting time of 10–20 s. The analytical beam diameter was 1 µm for solid inclusion mineral and 10 µm for chromite, respectively. Synthetic oxides and natural minerals were utilized as standards. The Fe²⁺ and Fe³⁺ contents in the chromite and clinopyroxene were calculated based on their ideal stoichiometries. The analytical results of the major elements for representative minerals are given in Supplementary Table S2. The compositional mappings of the solid inclusions were separately determined by energy dispersive X-ray spectroscopy using an accelerating voltage of 15 kV and a beam current of 10 nA.

Trace element analyses of chromite were conducted by LA-ICP-MS at the State Key Laboratory of Ore Deposit Geochemistry, Institute of Geochemistry Chinese Academy of Sciences. Laser sampling was performed using an ASI RESOLUTION-LR-S155 laser microprobe equipped with a Coherent Compex-Pro 193 nm ArF excimer laser. An Agilent 7700x ICP-MS instrument was used to acquire ion-signal intensities. Helium was applied as a carrier gas and mixed with argon via a T-connector before entering the ICP-MS.

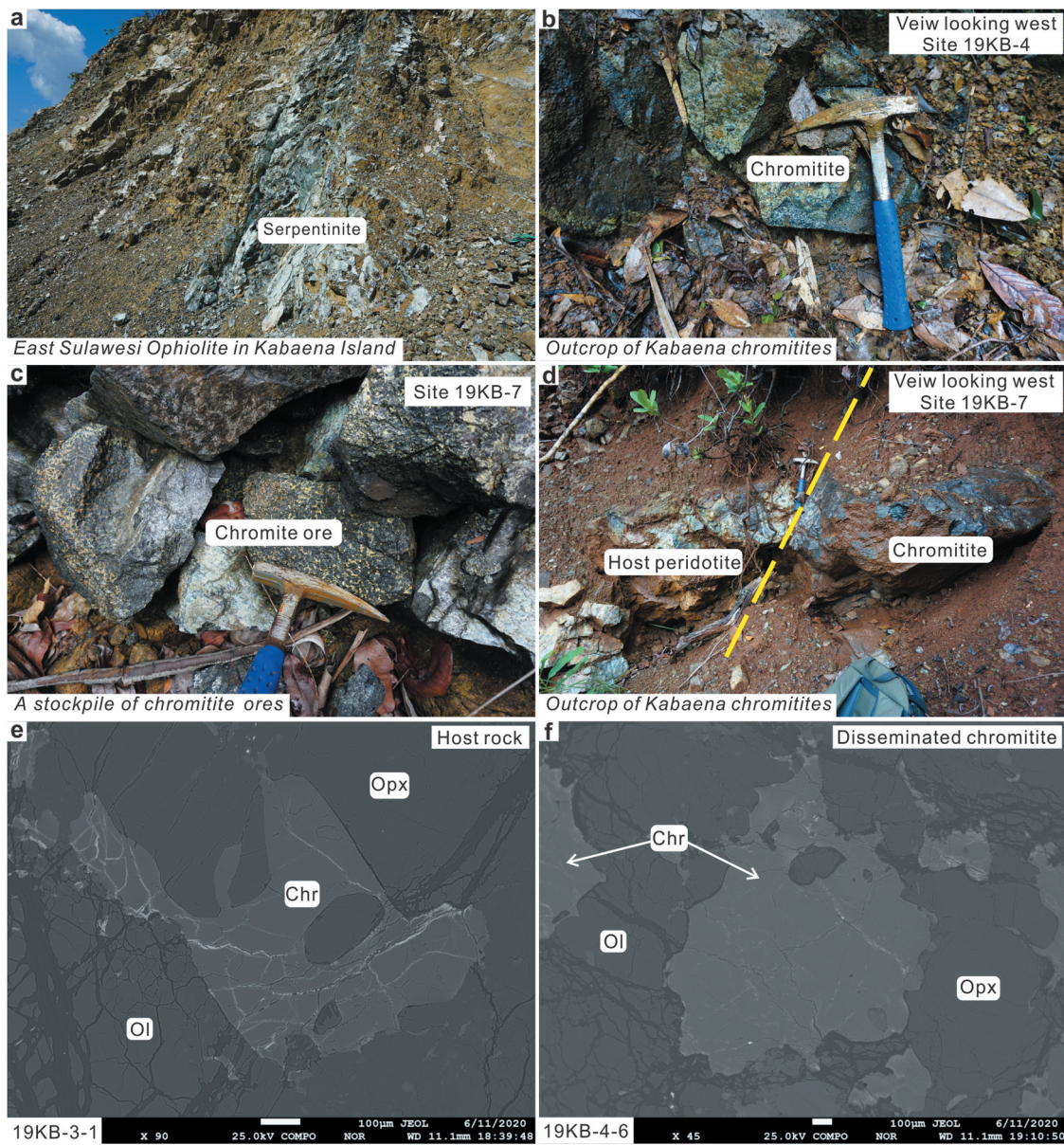


Figure 2. Representative photographs of field outcrops and mineral assemblages for the Kabaena chromitites and host peridotites. (a–d) Field photographs, and backscattered electron photographs of host peridotite (e) and disseminated chromitite (f). Chr = chromite, Ol = olivine, Opx = orthopyroxene.

The laser beam diameter was 40 μm for chromite. Each analysis incorporated a background acquisition of approximately 30s (gas blank) followed by 50s of data acquisition from the sample. Element contents were calibrated against multiple reference materials (GSE-1 G, BCR-2 G, BIR-1 G and BHVO-2 G) combined with internal standardization. The preferred values of element concentrations for the USGS reference glasses were obtained from the GeoReM database (<http://georem.mpch-mainz.gwdg.de>). Offline selection and integration of background and analyte signals, time-drift correction and quantitative calibration were performed using ICPMSDataCal (Liu *et al.* 2008).

The analytical results of the trace elements for chromite are given in Supplementary Table S2.

4. Mineral chemistry

4.1 Host peridotite

The Kabaena chromitites are mainly hosted in mantle harzburgite and lherzolite, but our chromitite samples were collected in harzburgite, which comprises olivine and orthopyroxene, with subordinate clinopyroxene and Cr-spinel (Figure 2e). The chemical compositions of these olivine crystals include

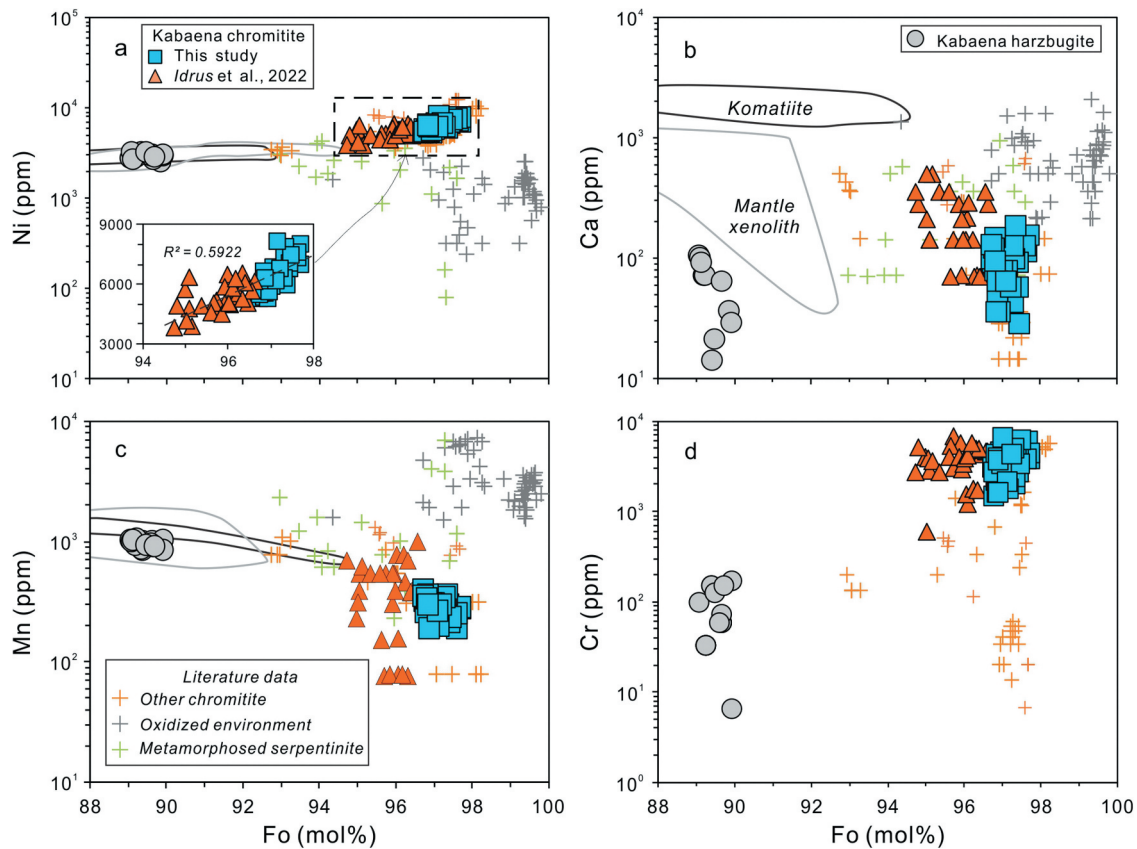


Figure 3. Forsterite (Fo) contents versus (a) Ni, (b) Mn, (c) Ca and (d) Cr contents of olivine from the Kabaena chromitites and host rocks. Olivine data for the other chromitites, the oxidized environment and the metamorphosed serpentinite are from the compiled database of Yao *et al.* (2021b). Olivine data for mantle xenoliths and komatiites are from Sobolev *et al.* (2007)

average values of ~90 Fo [100 Mg/(Mg + Fe), molar], ~3000 ppm Ni, <100 ppm Ca, and ~980 ppm Mn (Figure 3). Orthopyroxene is mainly composed of enstatite and pigeonite, with high Mg# [Mg/(Mg +

Fe²⁺), molar] values of ~0.91, 0.4–4.1 wt% CaO, and 4.8–6.2 wt% Al₂O₃. Clinopyroxene has a diopsidic composition, with an average value of ~0.95 Mg#, ~6.5 wt% Al₂O₃ and ~0.3 wt% Cr₂O₃ (Figure 4).

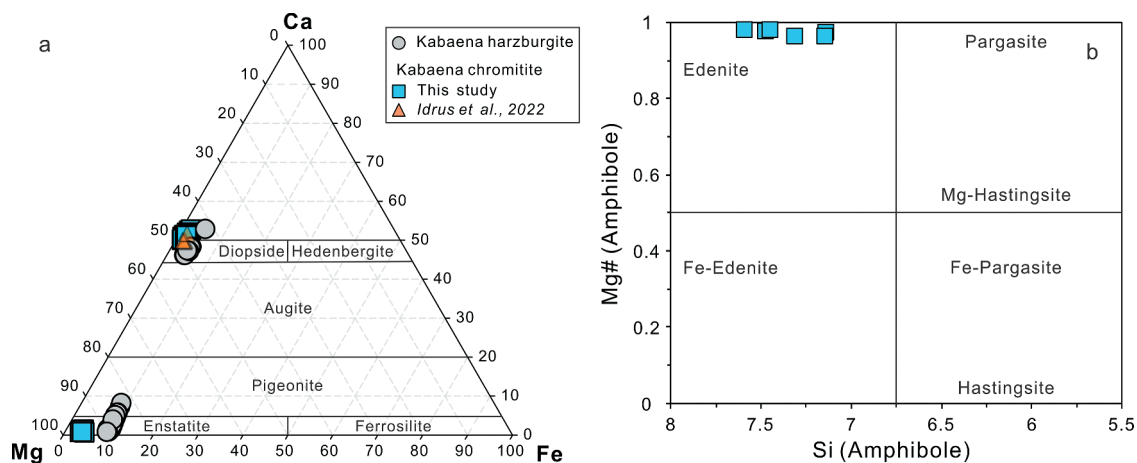


Figure 4. (a) The ternary diagram of Wo-En-Fs for primary pyroxene in chromitite and host harzburgite. (b) Mg# versus Si (a.p.f.u) for amphibole included in chromitite.

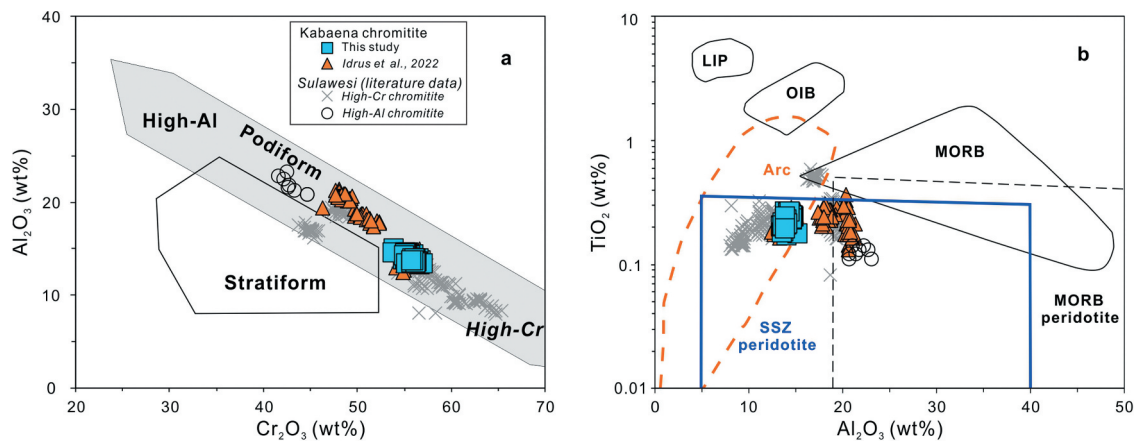


Figure 5. Composition of chromite plotted on Al₂O₃ versus Cr₂O₃ (a) and TiO₂ versus Al₂O₃ (b). The fields of podiform and stratiform chromitites in (a) are after Arai *et al.* (2004), and the fields in (b) are after Kamenetsky *et al.* (2001). The data for the high-Cr and high-Al chromitites in Sulawesi are from Zaccarini *et al.* (2016), Septiana *et al.* (2021) and Hasria *et al.* (2021). MORB: mid-ocean ridge basalt; SSZ: supra-subduction zone; LIP: large igneous province basalt; OIB: ocean island basalt; Arc: arc-related rock.

These mineral compositions are consistent with those of mantle harzburgites (Arai 1980; Khedr and Arai 2017; Pan *et al.* 2022).

4.2 Mineral chemistry of chromite

More than 60 microprobe analyses were obtained on the primary chromite core from the Kabaena chromitites. The compositions of the chromite grains vary only slightly, with 53.7–56.9 wt% Cr₂O₃, 13.4–15.1 wt% Al₂O₃, 9.7–11.7 wt% FeO, 2.8–4.3 wt% Fe₂O₃, 14.5–16.0 wt% MgO, and 0.17–0.27 wt% TiO₂. Based on the high Cr# values from 0.70 to 0.74 and high Mg# values from 0.69 to 0.75, the chromitites from disseminated, net-texture, and massive ores are categorized as high-Cr chromitites. In the diagram of Cr₂O₃–Al₂O₃ in chromite (Bonavia *et al.* 1993), the Kabaena chromitites and other chromitites hosted in the ESO plot within the ophiolitic podiform-type chromitite field (Figure 5a). The low TiO₂ and moderate Al₂O₃ contents of these chromitites are different from those of large igneous provinces (LIP), oceanic island basalts (OIB), mid-ocean ridge basalts (MORB) and MORB peridotites but resemble those from arc basalts (Kamenetsky *et al.* 2001). These results indicate that their parental melts are more likely to be well connected with arc-related rocks (Figure 5b).

The concentrations of Ni, Zn, V, Co, Sc and Ga in the Kabaena chromitites range from 760 to 1280 ppm, 441 to 616 ppm, 580 to 740 ppm, 160 to 210 ppm, 4.5 to 6.0 ppm, and 20.0 to 5.0 ppm, respectively. Bivariate diagrams of various trace element concentrations against Cr# of chromite minerals compare the Kabaena chromitites with ophiolitic high-Al chromitites, other ophiolitic high-Cr chromitites, layered intrusions and komatiites

(González-Jiménez *et al.* 2017 and references therein). The results are consistent with the signatures of high-Cr ophiolitic chromitites (Figure 6). In particular, the low Ga content in high-Cr ophiolitic chromitites is a remarkable geochemical feature that differentiates these chromitites from those with other origins (Figure 6f).

4.3 Solid inclusions hosted in the chromite

Silicate inclusions contain mainly olivine, pyroxene, and amphibole (Figure S1a–f). They are several tens of micrometres in size and are characterized by higher Mg/Fe ratios than the host rocks. Olivine inclusions exhibit extremely high Ni (5300 to 8200 ppm) and Cr (1500 to 6700 ppm) contents and low Ca (<200 ppm) and Mn (190 to 400 ppm) contents (Figure 3), as well as higher Fo (96.7 to 97.7 mol%) than those reported by Idrus *et al.* (2022). The Ni contents in the olivine inclusions are positively correlated with the Fo values.

Both orthopyroxene and clinopyroxene inclusions occur either as single crystals or paragenetic aggregates, which are composed of enstatite and diopside (Figure 4a). The average Mg#, Al₂O₃ and TiO₂ values of enstatite are ~96, 2.12 wt% and 0.08 wt%, respectively. The Mg# values of the diopside inclusions (0.96–0.99) are higher than those of enstatite, with average contents of 0.88 wt% Al₂O₃. Ellipsoidal chromites are found in silicate inclusions, indicating that they are primitive minerals of magmatic origin (Figure S1f). The amphibole inclusions are composed of 2.6 to 6.2 wt% Al₂O₃, 12.6 to 12.9 wt% CaO, 0.6 to 1.5 wt% Na₂O, 1.3 to 3.0 wt% Cr₂O₃, and 0.92 to 0.97 Mg#, which are edenites in composition (Figure 4b).

Sulfide inclusions hosted in chromite, generally smaller than 10 μm in size, are found in the Kabaena chromitites. These sulfide inclusions contain base metal and

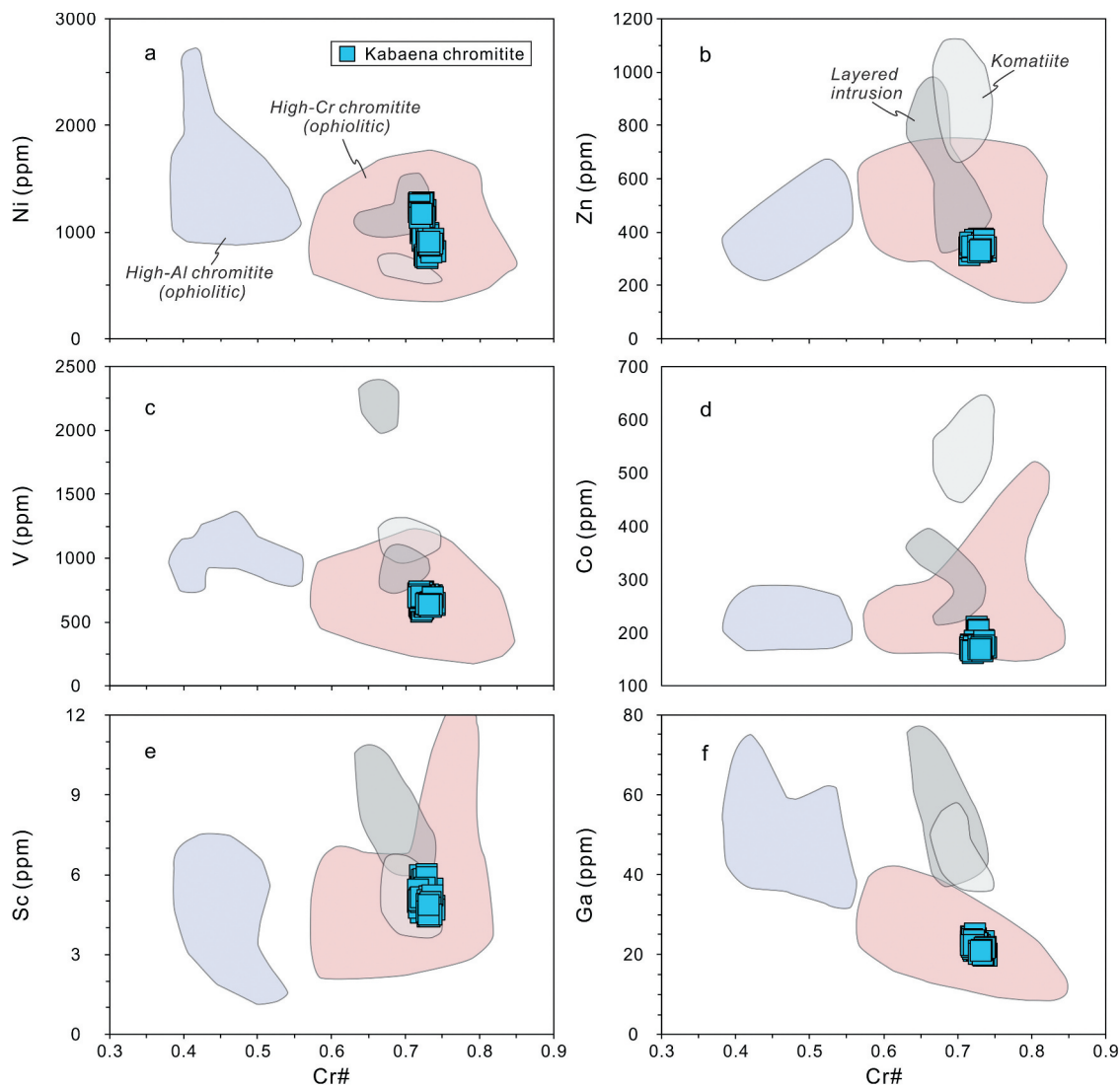


Figure 6. Variations in terms of Ni, Zn, V, Co, Sc and Ga vs. Cr# [Cr/(Cr + Al), molar] from the Kabaena chromitites. The fields are from González-Jiménez *et al.* (2017) and references therein.

platinum-group sulfides, occurring either as singular crystals or aggregates associated with silicates and/or other sulfides (Figure S1g–l). Millerite with euhedral–subhedral shapes is the most abundant BMS inclusion, with subordinate pentlandite and chalcopyrite. The Ni and Fe contents of millerites range from 57.1 to 62.8 wt% and 0.8 to 2.7 wt%, respectively. Pentlandite grains contain 44.3–47.1 wt% Ni and 16.2–20.6 wt% Fe. The PGE contents of the base metal sulfides are below the detection limits of EPMA.

Chromite-hosted platinum-group minerals (PGMs) are generally sulfide inclusions enriched in iridium subgroup PGEs (IPGE: Os, Ir, Ru). No PGE alloys or sulfide inclusions enriched in palladium subgroup PGEs (PPGE: Rh, Pt, Pd) were found. Five types of PGMs were distinguished in the thin sections. PGE sulfides of the laurite–

erlichmanite series are the most abundant phases. The second most common phase is Ir–Ni monosulfide, followed by a few irarsite and cuproiridsite phases. These PGM grains range from a few to several tens of micrometres in size and show euhedral, subhedral to anhedral shapes (Figure S1). They are usually found in aggregates but also rarely as single grains within chromite grains (Figure S2). Furthermore, the exsolution of various small PGM grains also occurs in some larger PGMs (Figure S1j–k). Laurites contain 31.5–16.8 wt% Ru and 10.3–22.2 wt% Os. Erlichmanites contain 11.3–21.5 wt% Ru and 36.2–44.5 wt% Os (Figure 7). Ir–Ni monosulfide grains contain 14.1–17.3 wt% Ni and 34.1–40.4 wt% Ir. The Ir and Cu contents of cuproiridsite are ~67.8 wt% and ~10.4 wt%, respectively. Irarsite (Irt) has ~41.6 wt% Ir, ~24.9 wt% Os and ~15.7 wt% As.

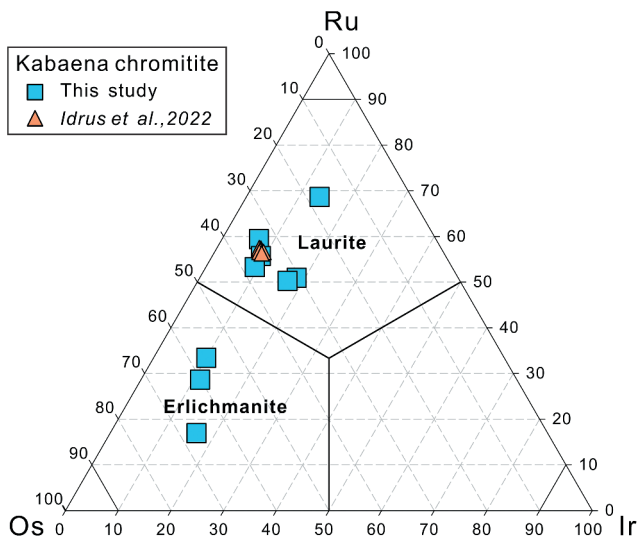


Figure 7. Ternary diagram of Ru-Os-Ir showing the composition of laurite-erlichmanite series minerals hosted in the chromite from the Kabaena chromitites.

Similarly, Uysal *et al.* (2009) also reported these solid inclusions of PGMs in the ophiolitic chromitites from the Muğla, SW Turkey.

5. Discussion

5.1 Nature of the parental magma of the Kabaena chromitites

In the chromite Cr# versus Mg# plot (Figure 8a), the Kabaena chromitites plot within the fields defined by Cr-spinel in boninites. The elevated Cr# and TiO₂ values in chromite also plot along the reaction trend of

harzburgite with boninitic melts (Figure 8b). These evidences imply a boninitic affinity for the Kabaena chromitites. Based on experiments and field studies, empirical equations of the Al₂O₃ and TiO₂ contents and FeO/MgO ratios have been established for chromite and the associated parental melts (Maurel 1984; Kamenetsky *et al.* 2001; Rollinson 2008; Zaccarini *et al.* 2011). The spinel–melt compositional relationship is independent of temperature variations. Zaccarini *et al.* (2011) used the data of Kamenetsky *et al.* (2001) to calibrate the relationship between the Al₂O₃ and TiO₂ contents of chromite and the parental melts. Massive and net-texture chromitites display a minimum subsolidus re-equilibration effect or post-cumulus reaction between the interstitial silicate and the chromite due to the higher proportion of chromite. We used the empirical equation of Zaccarini *et al.* (2011) and the chemical composition of the chromite core portion from the Kabaena massive and net-texture chromitites to estimate the Al₂O₃ and TiO₂ contents of the parental melts. The equations for the (TiO₂)_{melt} and (Al₂O₃)_{melt} in an arc setting are as follows:

$$(\text{Al}_2\text{O}_3)_{\text{melt}} = 5.2253 \times \ln(\text{Al}_2\text{O}_3)_{\text{spinel}} - 1.1232$$

$$(\text{TiO}_2)_{\text{melt}} = 1.0897 \times (\text{TiO}_2)_{\text{spinel}} + 0.0892$$

where Al₂O₃ and TiO₂ are in wt%. The calculated Al₂O₃ and TiO₂ contents of the parental melts for the Kabaena chromitites are 12.5–13.1 wt% and 0.25–0.39 wt%, respectively, which plot within the field of boninites (Figure 9a–c) and are far from the field of MORB. For comparison, the calculated parental melts of the high-Cr podiform chromitites in some typical ophiolites are

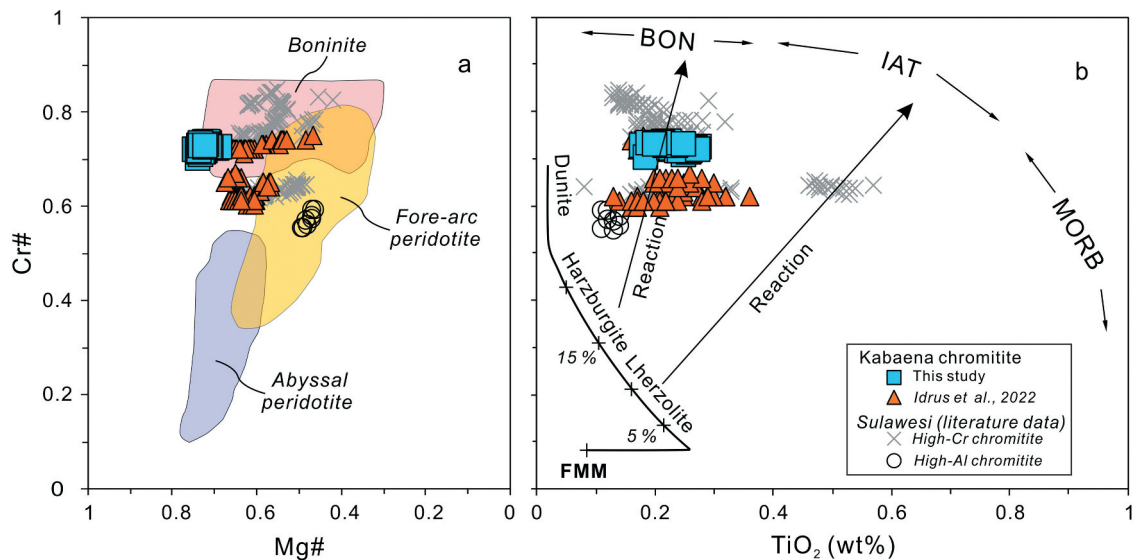


Figure 8. Composition of chromite plotted on Cr# versus Mg# (a) and Cr# versus TiO₂ (b) values. The fields in (a) and (b) are after Kamenetsky *et al.* (2001) and Tamura and Arai (2006). The Fertile MORB Mantle (FMM) is after Arai (1994). The data sources for the high-Cr and high-Al chromitites in Sulawesi are the same as in Figure 5.

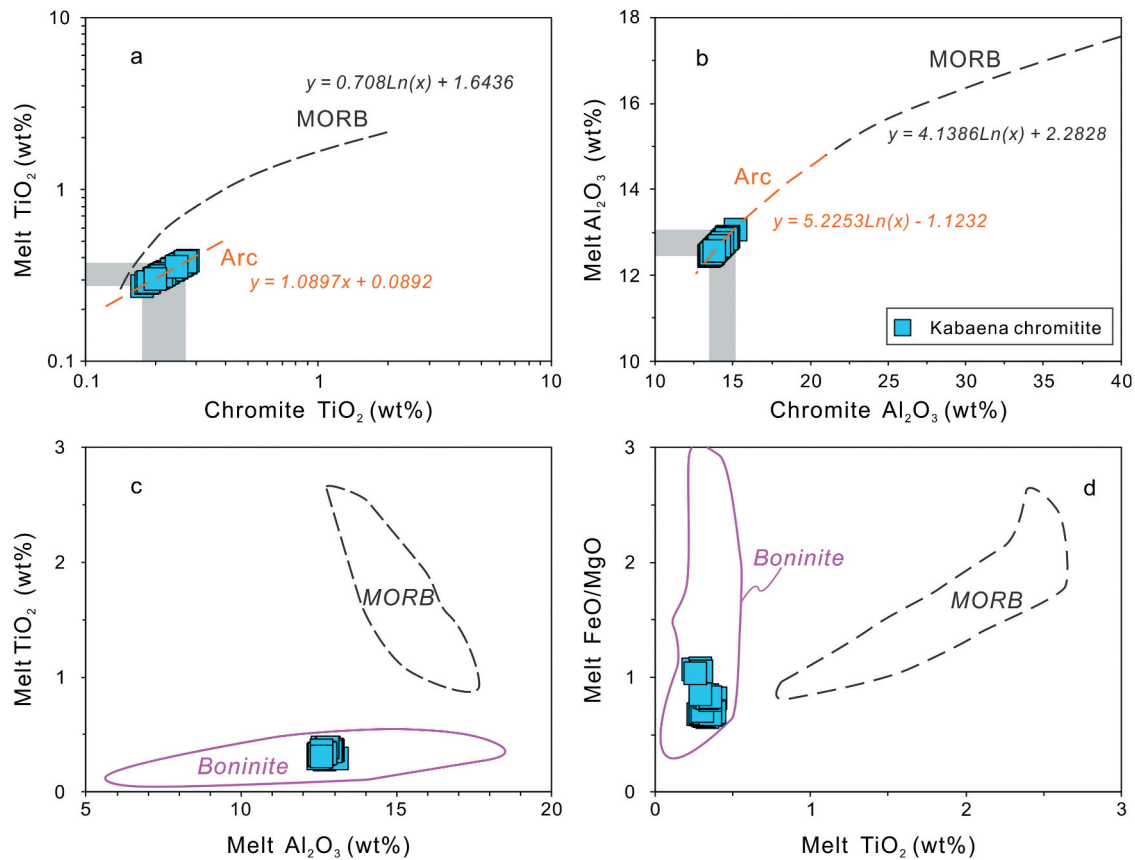


Figure 9. Calculated TiO_2 (a) and Al_2O_3 (b) contents of parent melts in equilibrium with the chromites from Kabaena. The melt TiO_2 , Al_2O_3 (c), and FeO/MgO (d) values of the Kabaena chromitites are compared with MORB (Gale *et al.* 2013) and boninitic compositions (GEOROCK database). The regression equations of Arc and MORB values are from Zaccarini *et al.* (2011)

summarized in Table S3. These data show that the Al_2O_3 and TiO_2 values of the parental melts of the Kabaena chromitites are in the range of the high-Cr chromitites from ophiolites [such as the ophiolites in Oman (Rollinson 2008), Elekdağ, Turkey (Dönmez *et al.* 2014) and Sagua de Tanamo, Cuba (González-Jiménez *et al.* 2011)] and typical boninites (Al_2O_3 : 5.8–18.0 wt% and TiO_2 : 0.07–0.6 wt%; Figure 9d). Additionally, the FeO/MgO ratios of the melts from which chromite crystallized were estimated using the empirical expression proposed by Maurel (1984):

$$\ln(\text{FeO/MgO})_{\text{spinel}} = 0.47 - 1.07 \times \text{Al}\#_{\text{spinel}} + 0.64 \times \text{Fe}\#_{\text{spinel}} + \ln(\text{FeO/MgO})_{\text{melt}}$$

where FeO and MgO are in wt%, $\text{Al}\# = \text{Al}/(\text{Cr} + \text{Al} + \text{Fe}^{3+})$ and $\text{Fe}\# = \text{Fe}^{3+}/(\text{Cr} + \text{Al} + \text{Fe}^{3+})$. The FeO/MgO ratios of the parental melts of the Kabaena chromitites vary from 0.66 to 0.82, and these values are comparable to those of the high-Cr ophiolitic chromitites in forearc and supra-subduction zone settings, such as the Santa Elena ophiolite (Zaccarini *et al.* 2011), the Nidar Ophiolite Complex, India (Nayak *et al.* 2021), the Elekdağ ophiolite, Turkey (Dönmez *et al.* 2014), and boninites (FeO/MgO : 0.3–2.9; Figure 9d).

Moreover, some selected major, minor, and trace elements of the chromites from the Kabaena chromitites were normalized to the composition of the MORB chromite and plotted following the order of elements suggested by Pagé and Barnes (2009). The results are compared with the values for chromite in boninitic lavas from the Thetford Mines Ophiolite (TMO) in Canada (Pagé and Barnes 2009), and chromite database for high-Cr chromitites and high-Al chromitites from Zhou *et al.* (2014). The MORB-normalized patterns of chromite grains from the Kabaena chromitites show slightly positive slopes from Al_2O_3 to Mn, with positive Ti and Mn anomalies and variable Sc contents, which are similar to those of boninitic lavas or ophiolitic high-Cr chromitites but different from those of high-Al chromitites (Figure 10). In addition, the existence of amphibole inclusions in the chromite suggests that the parental melts are rich in H_2O . This evidence suggests that the Kabaena high-Cr chromitites crystallized from boninitic melts in a subduction environment as opposed to MORB-like melts.

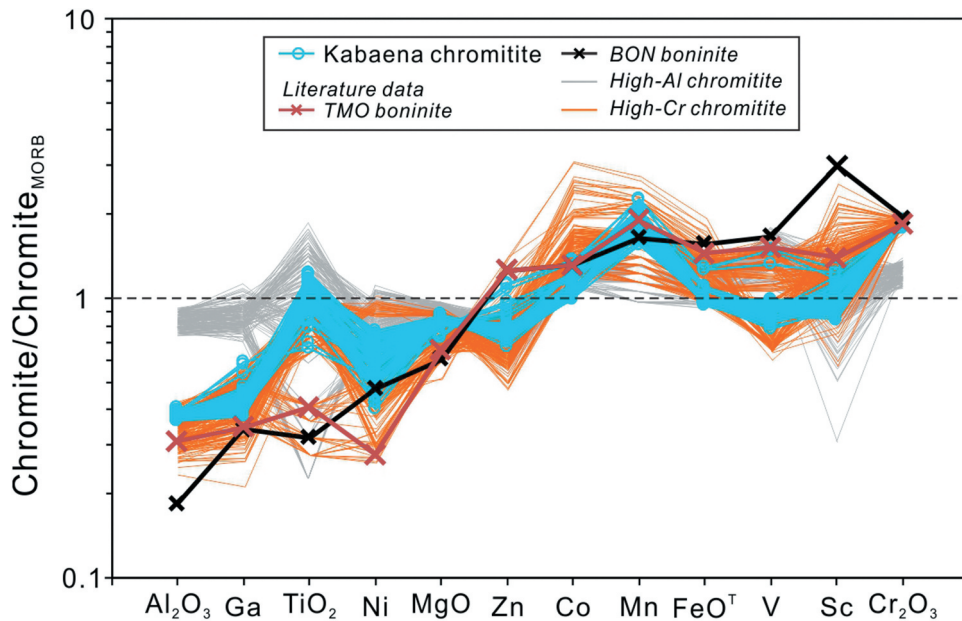


Figure 10. Chromite MORB-normalized major-trace element distribution of the Kabaena chromitites. Data source: normalized MORB values and TMO (Thetford Mines Ophiolite) boninite are from Pagé and Barnes (2009); high-Cr chromitites and high-Al chromitites are from Zhou *et al.* (2014)

5.2 Chromite-hosted solid inclusion constraints on physicochemical conditions

Solid inclusions hosted in chromite are enclosed during the growth of chromite crystals, which prevents further physicochemical exchange between these minerals and ambient melts. The compositions of these inclusions, therefore, can preserve several primitive pieces of information about the composition and physicochemical conditions of the parental melts from which they crystallized (Nayak *et al.* 2021; Sepidbar *et al.* 2021; Sideridis *et al.* 2021).

5.2.1 Silicate inclusion constraints on the temperature-pressure (T-P) conditions

Early studies proposed that ophiolitic chromitites could be formed under low-P conditions by the mixing of melts with different SiO₂ contents or the melt-rock reaction between mantle peridotite and melts (Arai 1994, 1997; Zhou *et al.* 1994). However, recent studies have shown that some ultrahigh-pressure (UHP) and highly reduced (HR) phase inclusions (e.g. CaFe₂O₄-phase, ringwoodite pseudomorph, diamond, Fe-silicides, carbide, native Fe and Si) are present in chromitites from Tibet, Urals, Myanmar and Oman (Robinson *et al.* 2004; Dobrzhinetskaya *et al.* 2009; Yamamoto *et al.* 2009; Yang *et al.* 2015; Pujol-Solà *et al.* 2020). Some researchers have suggested that the presence of UHP and HR minerals can be regarded as important evidence for the deep mantle origin of these chromitites (e.g. Dobrzhinetskaya

et al. 2009; Yang *et al.* 2015; Guo *et al.* 2021). However, other researchers have found that some HR/UHP minerals observed in ophiolitic chromitites can also be produced by the ocean-floor metamorphic processes of ultramafic/mafic rocks under low T-P conditions instead of those of deep mantle origin (Pujol-Solà *et al.* 2018, 2020, 2021; Farré-de-Pablo *et al.* 2019). Therefore, in order to determine if the chromitites formed at low- or high-pressure environments, or if they were recycled at high pressures, detailed mineralogical studies and T-P estimates are needed to determine the crystallization T-P environment for chromitites.

Unaltered clinopyroxene and orthopyroxene, as mineral pairs, often coexist and are included in the chromite from the Kabaena chromitites, indicating that they are primary inclusions in equilibrium with primitive magma. Putirka (2008) summarized and calibrated the geothermobarometry of the clinopyroxene-orthopyroxene Fe–Mg exchange, which has been widely used to estimate the T-P conditions of parental magma and mantle rocks (e.g. Perkins and Anthony 2011; Guo *et al.* 2021). Based on this geothermobarometry, the calculated T-P conditions of the parental magma of the Kabaena chromitites range from 950 to 1010°C and from 7.0 to 8.4 Kbar, respectively (Table S4), which are in line with the T-P conditions in the uppermost mantle. In addition, no diopside lamellae-bearing chromite (UHP minerals), diamond or native elements (HR minerals) were found in the Kabaena chromitites. Experiments (Liu and O’neill 2004; Zhang *et al.* 2017) have shown

that the Si and Ca contents in chromite are affected by ambient temperatures and pressures, which can cause variations of a few thousand ppm. The lower Si contents (500–950 ppm) of the Kabaena chromitites relative to those from Luobusa ophiolites (500–10,000 ppm; Su *et al.* 2019) are consistent with an origin at a shallow depth. Therefore, our data indicate that the Kabaena chromitites were formed at shallow mantle depths (e.g. the Moho Transition Zone and the upper-most mantle).

5.2.2 Sulfide inclusion constraints on sulphur fugacity conditions

In the high-Cr chromitites from Kabaena Island, Southeast Sulawesi, some euhedral-subhedral sulfide inclusions are enclosed in unaltered chromite grains away from cracks and fractures. This observation indicates that the sulfide grains formed at or before chromite crystallization and were not affected by post-magmatic hydrothermal alteration after their entrapment in chromite. In agreement with other high-Cr ophiolitic chromitites (e.g. Bou Azzer chromitites, Pujol-Solà *et al.* 2021; southeastern Turkey chromitites, Akmaz *et al.* 2014; Eastern Cuba chromitites, Gervilla *et al.* 2005), the results of this study and recent research by Idrus *et al.* (2022) show that PGMs in the Kabaena chromitites are characterized by IPGE-bearing (Os–Ru–Ir) sulfides, such as laurite, erlichmanite, and irarsite, whereas no PPGE-bearing (Pd–Pt–Rh) minerals have been found. The presence of exclusive IPGE-bearing PGMs implies that the parental magmas are enriched in IPGE but depleted in PPGE. During the process of the partial melting of mantle peridotites, refractory IPGE are often trapped in residual sulfides or PGM in the mantle, while the more mobile PPGE are transferred to silicate melt (Bockrath *et al.* 2004). In other words, the parental magmas with IPGE enrichment and PPGE depletion in the Kabaena chromitites were derived from a depleted mantle that experienced melting events. The melts produced at the early stage extracted the PPGE in the mantle, resulting in the formation of depleted mantle mainly containing IPGE. Additionally, in the Kabaena chromitites, four other pieces of evidence support the depleted features of the mantle: (1) mantle harzburgite is the host rock; (2) the Cr# values of the chromite grains are higher than those of abyssal peridotite (Figure 8a); (3) in the chromite TiO₂ vs. Cr# plot, the chromites plot on the trend line of the reaction between harzburgite and boninitic melts (Figure 8b); and (4) all the silicate inclusions in the chromites have higher Mg# or Fo values than the host harzburgites (Figures 3–4). Therefore, we propose that the Kabaena chromitites have a close genetic relationship with depleted mantle (such as harzburgite).

Furthermore, Brenan and Andrews (2001) and Andrews and Brenan (2002) used experimental results to evaluate the effects of temperature (T) and $f(S_2)$ on phase relations in the Ru–Os–Ir–Ni–S system and established the corresponding relationship between them. At high temperatures and low $f(S_2)$ values (1200–1300°C and $\log f(S_2)$ from 2 to 1.3), Os–Ir alloys and the end member composition of RuS₂ (very low contents of Os and Ir) prefer to crystallize. As the $f(S_2)$ value increases and the temperature decreases, laurite can progressively accommodate more Os because the partition coefficient of Os significantly increases between laurite and silicate melt (Brenan and Andrews 2001; Andrews and Brenan 2002). Considering that Ir–Os alloys are associated with awaruites in the serpentine gangue of the Kabaena chromitites, Idrus *et al.* (2022) suggested that they were secondary exsolution products at ~400°C. Similarly, no Os–Ir alloy inclusions were found in this study. The investigated laurite inclusions in the Kabaena chromitites feature Os enrichment (10–22 wt %). Several euhedral erlichmanite grains were also found in the chromite, instead of Os–Ir alloys. These assemblages indicate that the Kabaena chromitites started to form at lower temperatures but slightly higher $f(S_2)$ values than those defined by Brenan and Andrews (2001) for the stability of laurite (1100–1200°C). With the constant increase in the $f(S_2)$ value and the decrease in temperature, erlichmanite continued to crystallize. Irarsite is attached to the outer envelope of laurite-erlichmanite, showing that arsenic activity increases after the crystallization of laurite. Subsequently, the

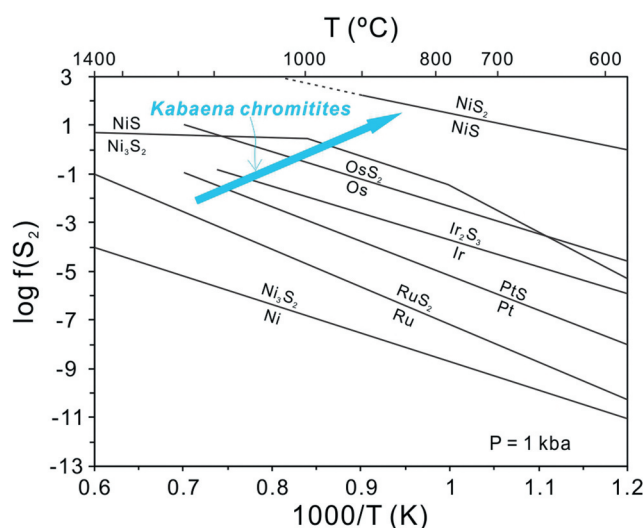


Figure 11. Metal-sulfide equilibrium lines for Ru, Pt, Ir, Os and Ni as a function of sulphur fugacity [$\log f(S_2)$] and temperature (T) (modified from Melcher *et al.* 1997). The blue arrow shows the crystallization trend of $f(S_2)$ -T for the Kabaena chromitites.

PGMs of cuproiridsite and Ir–Ni monosulfide may crystallize. The presence of millerite (NiS) inclusions in the chromite further indicates that the crystallization conditions of the Kabaena chromitite are beyond the heazlewoodite (Ni₃S₂)–millerite (NiS) buffer and include lower temperatures (down to 864°C) and higher $f(S_2)$ conditions (Figure 11; Melcher *et al.* 1997). Base metal sulfide inclusions of rare pentlandite and chalcopyrite in chromite correspond to late crystallized phases after the formation of PGM assemblages when the temperature dropped and the $f(S_2)$ value increased further. Therefore, the BMS and PGM assemblages reveal that the parental magmas for the Kabaena chromitites experienced an evolutionary process from high T and low $f(S_2)$ conditions at the early stage to low T and high $f(S_2)$ conditions at the late stage.

5.3 Origin of high-Ni-Cr extreme-Mg olivine inclusions hosted in chromite

Plechov *et al.* (2018) and Yao *et al.* (2021b) summarized the structure and chemical compositional characteristics of extreme-Mg olivine (Fo >96) with different origins, including skarn xenoliths, carbonate-related alkaline volcanic rocks, metamorphosed serpentinites, oxidized environments, and chromitite ores. In the Kabaena chromitites, extreme-Mg olivines are present as inclusions hosted in chromite grains. No skarn xenoliths or carbonate-related components were found based on detailed observations of thin sections. The Ni and Mn contents of extreme-Mg olivines from metamorphosed serpentinites are similar to those of olivines from mantle xenoliths and komatiites (Khedr and Arai 2012), and olivines from oxidized environments show exsolution lamella of iron oxide (Plechov *et al.* 2018). However, the extreme-Mg olivine from the Kabaena chromitites has very high Ni and Cr contents, which resembles extreme-Mg olivines from other chromitites (e.g. Luobusa, Xiong *et al.* 2015; Su *et al.* 2019; Ray-Iz, Plechov *et al.* 2018). Subsolidus re-equilibration of Fe–Mg exchange between chromite and olivine inclusions may provide an accepted mechanism that elevates the Fo content of olivine when they come in contact (Yang *et al.* 2015; Bai *et al.* 2017), but the genesis of extreme-Mg olivine inclusions for chromitite ore has not been well constrained.

Euhedral mineral inclusions are often regarded as earlier crystalline minerals from primitive magma relative to host minerals. Extreme-Mg olivine inclusions in the Kabaena chromitites are plentiful and euhedral-subhedral in shape. Namely, we should first consider the possibility of magmatic origin for these extreme-Mg olivines. As shown in Figure 3, olivine with Fo >96 is difficult to be produced by normal mantle-derived melts that are

even derived from high-degree mantle melting (e.g. komatiites). Yao *et al.* (2021b) proposed that extreme-Mg olivine can crystallize from primitive Mg-rich carbonate melt under high oxygen fugacity (fO_2) conditions. Because high fO_2 can convert Fe²⁺ into Fe³⁺, it no longer fits into the octahedral site. Additionally, in the oxygen fugacity (fO_2) experimental data reported by Blundy *et al.* (2020), extreme-Mg olivines were found in the high fO_2 samples ($\log fO_2 > -2.9$), indicating that high fO_2 conditions can be a controlling factor for the crystallization of magmatic extreme-Mg olivine. However, the presence of numerous sulfide inclusions implies that the parental magma of the Kabaena chromitites is under a relatively reduced environment and prevents the model of magmatic origin for Kabaena extreme-Mg olivine. Compiled olivine data show that chromite-hosted olivine has extremely high Fo contents and very high Cr and Ni contents. Bai *et al.* (2017) performed compositional profile analyses of chromite and olivine and found that the FeO content in the part of the olivine that was in contact with the rim of the chromite was lower. Xiao *et al.* (2016) reported a positive correlation between the olivine $\delta^{56}\text{Fe}$ values and the Fo contents in Luobusa harzburgite-dunite-chromitite. These results confirm the occurrence of Fe–Mg exchange between chromite and olivine, namely, Fe from olivine to chromite and Mg from chromite to olivine, which may have elevated the Fo contents of olivine. Bai *et al.* (2017) suggested that the mechanism of Fe–Mg exchange can cause the decoupling of the Fo and Ni contents in olivine. However, the Ni contents in extreme-Mg olivine from the Kabaena chromitites are positively correlated with the Fo contents, with $R^2 = 0.6$ (Figure 3a). This finding indicates that Fe–Ni exchange may also exist in olivine–chromite, which may be an analogous mechanism to the Fe–Ni exchange reaction of olivine–sulfide that occurs widely in magmatic Cu–Ni sulfide deposits (e.g. Li *et al.* 2007; Yao *et al.* 2018). Therefore, the Fe–Mg and Fe–Ni exchanges between olivine and chromite are the key factors causing the extremely high Ni and Fo contents in the olivine inclusions from the Kabaena chromitites.

Additionally, the high Cr content in extreme-Mg olivine associated with chromitite is another outstanding feature, but the factor causing it is still uncertain. Because trivalent cations do not prefer to partition into olivine, experiments of element diffusion in olivine and chromite (Spandler *et al.* 2007) showed that their diffusion is generally slower than that of divalent cations in olivine. Pagé and Barnes (2009) estimated the correlations between the proportion of chromite in whole rock and the concentrations of minor and trace elements in chromites for podiform chromitites from Thetford Mines Ophiolite. These correlations indicated that the Cr, Ti, Ga, and V contents in chromite were not easily modified by

re-equilibration reactions with olivine during cooling and could preserve the early magmatic signature. Our preceding discussion shows that the Kabaena high-Cr chromitites have a close genetic relationship with boninitic melts. Primitive boninitic melts are known to be richer in Cr (up to 4890 ppm; Walker and Cameron 1983; Pearce *et al.* 1992;) than other mantle-derived primitive basaltic melts (~200 to 500 ppm Cr; Roeder *et al.* 2006). Therefore, we suggest that the extreme-Mg olivine inclusions in the Kabaena chromitite crystallized from high-Mg and Cr boninitic melts in the early stages. Subsequently, subsolidus re-equilibration (Fe–Mg and Fe–Ni exchange) between the chromite and the olivine further increased the Ni and Fo contents of the olivine hosted in the chromite during cooling.

5.4 Genesis of podiform chromitites in Sulawesi and tectonic implications

Different models for the formation of podiform chromitites have been proposed, mainly including fractional crystallization of basaltic melts (Lago *et al.* 1982), mantle residue after high-degree melting (Wang and Bao 1987), melt-peridotite reactions (Arai and Yurimoto 1994; Zhou *et al.* 1994), deep mantle recycling (Arai 2013), mantle plume (Xiong *et al.* 2015; Yang *et al.* 2015), and melt-fluid immiscibility (Su *et al.* 2020). Given that our results for the high-Cr podiform chromitites from Kabaena Island, Southeast Sulawesi are more consistent with the melt-rock reaction model, we suggest that they were formed by the interaction of boninitic melts and depleted mantle (harzburgite) at the depth of the Moho transition zone or the uppermost mantle in the SSZ environment. This mechanism has also been widely used to explain the formation of other high-Cr podiform chromitites around the globe (e.g. Uysal *et al.* 2009; González-Jiménez *et al.* 2011). High-Al and high-Cr chromitite deposits have been reported in the ESO of Sulawesi, Indonesia (Zaccarini *et al.* 2016; Hasria *et al.* 2021; Septiana *et al.* 2021). The high-Al chromitites are considered to have crystallized from high-Al magmas that were produced by the fractional evolution of initial high-Cr boninitic magmas (Zaccarini *et al.* 2016), which is different from the more pervasive origin related to the MORB-like or arc tholeiitic magma. The palaeogeographic reconstruction indicated that the ESO, long with Ontong-Java and Hess Rise, was initially formed near the large composite mass of oceanic plateaus and seamounts by the SW Pacific Superplume at ~137 Ma (e.g. Parkinson 1998; Kadarusman *et al.* 2004). Subsequently, the ESO moved westward and accreted onto the Sundaland continental margin at ~30 Ma due to the birth of a fast-spreading mid-oceanic ridge. In the Miocene (~20 Ma), some microcontinental fragments

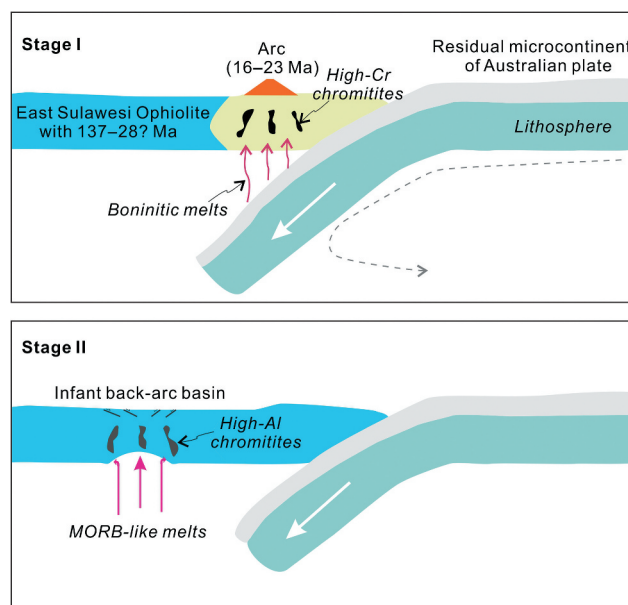


Figure 12. Schematic geodynamic setting for the formation of the high-Cr and high-Al podiform chromitites in the East Sulawesi Ophiolite. Age data are from Kadarusman *et al.* (2004)

from the Indo-Australian Plate (e.g. the Banggai-Sula and Tukang-Besi microcontinents) started to subduct westward beneath the ESO. This new subduction zone was recorded by the numerous arc-type Neogene volcanoclastic basalts (NVC; 23–16 Ma) covering the ESO (Kadarusman *et al.* 2004). Meanwhile, our results also indicate that the formation of high-Cr podiform chromitites in Kabaena has a close genetic relationship with boninitic melts. Together with the presence of hydrous silicate minerals (amphibole), boninitic melts in the Kabaena chromitites can be used to infer the initiation of a new subduction zone. Considering that the compositions of high-Al chromites (such as intermediate $Mg^{\#}$ and $Cr^{\#}$ values, and low TiO_2 contents) in Sulawesi are similar to those from SSZ peridotite (Figures 5b and 8), they most likely formed in MORB-like magmas in a back-arc setting. Another alternative genesis model for Sulawesi chromitites is shown in Figure 12. In the first stage, the high-Cr chromitites were formed by the reaction of depleted mantle and boninitic magma beneath a juvenile island arc; in the second stage, the high-Al chromitites were produced by the reaction of less depleted mantle and MORB-like magma in a transitional geotectonic environment from the arc to back-arc setting. The chromitite deposits in the Kabaena Island and Southeast Arm of Sulawesi (Figure 1), close to the subduction zone, record high-Cr compositional features related to boninitic magma, whereas those of the South Arm (Figure 1), away from the subduction zone, show a transition from high-Cr to high-Al compositions in

a back-arc setting. Thus, similar to podiform chromitites from southeastern Turkey and eastern Cuba ophiolites (Gervilla *et al.* 2005; Akmaz *et al.* 2014), we suggest that the cooccurrence of high-Al as well as high-Cr chromitites in Sulawesi may be a response to tectonic evolution from subduction initiation to the back-arc basin since the Miocene.

6. Conclusions

The podiform chromitites from Kabaena Island, Southeast Sulawesi, are high in Cr# (0.70 to 0.74) and contain massive, net-texture, and disseminated ores. Here, we first conduct a systematic study of mineral chemistry. These data and a compilation of previously published data for the ESO allow us to draw the following conclusions:

- (1) The major and trace element compositions of chromite and the estimated Al_2O_3 and TiO_2 contents and FeO/MgO ratios of parental melt for the Kabaena chromitites imply that they were formed by the reaction of boninitic melts and depleted mantle (harzburgite).
- (2) The estimated T-P conditions of the parental magma of the Kabaena chromitites are 950–1010°C and 7.0–8.4 Kbar, indicating that they were more likely formed in the uppermost mantle.
- (3) The sulfide assemblage of laurite-erlichmanite-irarsite-millerite reveals that the parental magmas for the Kabaena chromitites experienced an evolution of high T and low $f(S_2)$ to low T and high $f(S_2)$ from the early to late stage.
- (4) Based on the composition of extreme-Mg olivine inclusions in chromite and comparison with other extreme-Mg olivines from different environments, we propose that they crystallized from high-Cr boninitic melts and then further increased Fo contents by subsolidus re-equilibration (Fe–Mg and Fe–Ni exchange) with chromite.
- (5) Combined with the palaeogeographic reconstruction and reported data for podiform chromitites in the ESO of Sulawesi, we suggest that the cooccurrence of high-Al and high-Cr chromitites in this region could imply a tectonic evolution from subduction initiation to a back-arc basin.

Acknowledgments

We are grateful to Editor Robert J. Stern for efficient editorial handling and constructive comments, and two anonymous reviewers for their insightful suggestions and

comments that have greatly improved the manuscript. We thank Xiang Li and Wenqin Zheng for EMPA mineral major oxide analyses and Zhihui Dai for LA-ICP-MS mineral trace element analyses

Disclosure statement

No potential conflict of interest was reported by the author(s).

Funding

This work was financially supported by the Research Fund for the Doctoral Program of Tongren University (No. trxyDH2016), the Natural Science Foundation of China (NSFC Nos. 42206051, U1603245 and 41703051), the Natural Science Foundation of Shandong Province (No. ZR2020MD070), the Chinese Academy of Sciences—Light of West China Program, and the Natural Science Foundation of Guizhou Province (No. [2018] 1171).

ORCID

Chengquan Wu  <http://orcid.org/0000-0002-8017-7185>

References

- Akmaz, R.M., Uysal, I., and Saka, S., 2014, Compositional variations of chromite and solid inclusions in ophiolitic chromitites from the southeastern Turkey: Implications for chromite genesis: *Ore Geology Reviews*, v. 58, p. 208–224. [10.1016/j.oregeorev.2013.11.007](https://doi.org/10.1016/j.oregeorev.2013.11.007)
- Andrews, D.R., and Brenan, J.M., 2002, Phase-equilibrium constraints on the magmatic origin of laurite + Ru–Os–Ir alloy: *The Canadian Mineralogist*, v. 40, no. 6, p. 1705–1716. [10.2113/gscanmin.40.6.1705](https://doi.org/10.2113/gscanmin.40.6.1705)
- Arai, S., 1980, Dunite—harzburgite—chromitite complexes as refractory residue in the Sangun—Yamaguchi zone, western Japan: *Journal of Petrology*, v. 21, no. 1, p. 141–165. [10.1093/ptrology/21.1.141](https://doi.org/10.1093/ptrology/21.1.141)
- Arai, S., 1994, Characterization of spinel peridotites by olivine-spinel compositional relationships: Review and interpretation: *Chemical Geology*, v. 113, no. 3–4, p. 191–204. [10.1016/0009-2541\(94\)90066-3](https://doi.org/10.1016/0009-2541(94)90066-3)
- Arai, S., 1997, Origin of podiform chromitites: *Journal of Asian Earth Sciences*, v. 15, No. 2–3, p. 303–310
- Arai, S., 2013, Conversion of low-pressure chromitites to ultrahigh-pressure chromitites by deep recycling: A good inference: *Earth and Planetary Science Letters*, v. 379, p. 81–87. [10.1016/j.epsl.2013.08.006](https://doi.org/10.1016/j.epsl.2013.08.006)
- Arai, S., Uesugi, J., and Ahmed, A. H., 2004, Upper crustal podiform chromitite from the northern Oman ophiolite as the stratigraphically shallowest chromitite in ophiolite and its implication for Cr concentration: *Contributions to Mineralogy and Petrology*, v. 147, no. 2, p. 145–154. [10.1007/s00410-004-0552-8](https://doi.org/10.1007/s00410-004-0552-8)
- Arai, S., and Yurimoto, H., 1994, Podiform chromitites of the Tari-Misaka ultramafic complex, southwestern Japan, as mantle-melt interaction products: *Economic Geology*, v. 89, no. 6, p. 1279–1288. [10.2113/gsecongeo.89.6.1279](https://doi.org/10.2113/gsecongeo.89.6.1279)

- Bai, Y., Su, B.-X., Chen, C., Yang, S.-H., Liang, Z., Xiao, Y., Qin, K.-Z., and Malaviarachchi, S.P., 2017, Base metal mineral segregation and Fe-Mg exchange inducing extreme compositions of olivine and chromite from the Xiadong Alaskan-type complex in the southern part of the Central Asian Orogenic Belt: *Ore Geology Reviews*, v. 90, p. 184–192. [10.1016/j.oregeorev.2017.01.023](https://doi.org/10.1016/j.oregeorev.2017.01.023)
- Bao, P.-S., 2009, Further discussion on the genesis of the podiform chromite deposits in the ophiolites—questioning about the rock/melt interaction metallogeny: *Geological Bulletin of China*, v. 28, p. 1941–1961
- Barnes, S.J., and Roeder, P.L., 2001, The range of spinel compositions in terrestrial mafic and ultramafic rocks: *Journal of Petrology*, v. 42, no. 12, p. 2279–2302. [10.1093/petrology/42.12.2279](https://doi.org/10.1093/petrology/42.12.2279)
- Bergman, S.C., Coffield, D.Q., Talbot, J.P., and Garrard, R.A., 1996, Tertiary tectonic and magmatic evolution of western Sulawesi and the Makassar Strait, Indonesia: Evidence for a Miocene continent-continent collision: *Geological Society, London, Special Publications*, v. 106, no. 1, p. 391–429. [10.1144/GSL.SP.1996.106.01.25](https://doi.org/10.1144/GSL.SP.1996.106.01.25)
- Blundy, J., Melekhova, E., Ziberna, L., Humphreys, M.C., Cerantola, V., Brooker, R.A., McCammon, C.A., Pichavant, M., and Ulmer, P., 2020, Effect of redox on Fe–Mg–Mn exchange between olivine and melt and an oxybarometer for basalts: *Contributions to Mineralogy and Petrology*, v. 175, no. 11, p. 1–32. [10.1007/s00410-020-01736-7](https://doi.org/10.1007/s00410-020-01736-7)
- Bockrath, C., Ballhaus, C., and Holzheid, A., 2004, Stabilities of laurite RuS_2 and monosulfide liquid solution at magmatic temperature: *Chemical Geology*, v. 208, no. 1–4, p. 265–271. [10.1016/j.chemgeo.2004.04.016](https://doi.org/10.1016/j.chemgeo.2004.04.016)
- Bonavia, F., Diella, V., and Ferrario, A., 1993, Precambrian podiform chromitites from Kenticha Hill, southern Ethiopia: *Economic Geology*, v. 88, no. 1, p. 198–202. [10.2113/gsecongeo.88.1.198](https://doi.org/10.2113/gsecongeo.88.1.198)
- Brenan, J.M., and Andrews, D., 2001, High-temperature stability of laurite and Ru–Os–Ir alloy and their role in PGE fractionation in mafic magmas: *The Canadian Mineralogist*, v. 39, no. 2, p. 341–360. [10.2113/gscanmin.39.2.341](https://doi.org/10.2113/gscanmin.39.2.341)
- Dobrzhinetskaya, L.F., Wirth, R., Yang, J., Hutcheon, I.D., Weber, P.K., and Green, H.W., 2009, High-pressure highly reduced nitrides and oxides from chromite of a Tibetan ophiolite: *Proceedings of the National Academy of Sciences*, v. 106, p. 19233–19238. [10.1073/pnas.0905514106](https://doi.org/10.1073/pnas.0905514106)
- Dönmez, C., Keskin, S., Günay, K., Çolakoğlu, A.O., Çiftçi, Y., Uysal, İ., Türkel, A., and Yıldırım, N., 2014, Chromite and PGE geochemistry of the Elekdağ Ophiolite (Kastamonu, Northern Turkey): Implications for deep magmatic processes in a supra-subduction zone setting: *Ore Geology Reviews*, v. 57, p. 216–228. [10.1016/j.oregeorev.2013.09.019](https://doi.org/10.1016/j.oregeorev.2013.09.019)
- Fadhlurrohman, I., Parma, A.F., and Fitriani, C., 2017, Geological observation on Kabaena island, southeast Sulawesi: An implication of hydrocarbon occurrence in a frontier area based on outcrop study.
- Farré-de-pablo, J., Proenza, J.A., González-Jiménez, J.M., García-Casco, A., Colás, V., Roqué-Rossell, J., Camprubí, A., and Sánchez-Navas, A., 2019, A shallow origin for diamonds in ophiolitic chromitites: *Geology*, v. 47, no. 1, p. 75–78. [10.1130/G45640.1](https://doi.org/10.1130/G45640.1)
- Gale, A., Dalton, C.A., Langmuir, C.H., Su, Y., and Schilling, J.G., 2013, The mean composition of ocean ridge basalts: *Geochemistry: Geophysics, Geosystems*, v. 14, no. 3, p. 489–518. [10.1029/2012GC004334](https://doi.org/10.1029/2012GC004334)
- Gervilla, F., Proenza, J., Frei, R., Gonzalez-Jimenez, J.M., Garrido, C.J., Melgarejo, J., Meibom, A., Díaz-Martínez, R., and Lavaut, W., 2005, Distribution of platinum-group elements and Os isotopes in chromite ores from Mayarí-Baracoa Ophiolitic Belt (eastern Cuba: *Contributions to Mineralogy and Petrology*, v. 150, no. 6, p. 589–607. [10.1007/s00410-005-0039-2](https://doi.org/10.1007/s00410-005-0039-2)
- González-Jiménez, J.M., Camprubí, A., Colás, V., Griffin, W.L., Proenza, J.A., O'Reilly, S.Y., Centeno-García, E., García-Casco, A., Belousova, E., and Talavera, C., 2017, The recycling of chromitites in ophiolites from southwestern North America: *Lithos*, v. 294, p. 53–72. [10.1016/j.lithos.2017.09.020](https://doi.org/10.1016/j.lithos.2017.09.020)
- González-Jiménez, J., Proenza, J., Gervilla, F., Melgarejo, J., Blanco-Moreno, J., Ruiz-Sánchez, R., and Griffin, W., 2011, High-Cr and high-Al chromitites from the Sagua de Tánamo district, Mayarí-Cristal ophiolitic massif (eastern Cuba): Constraints on their origin from mineralogy and geochemistry of chromian spinel and platinum-group elements: *Lithos*, v. 125, no. 1–2, p. 101–121. [10.1016/j.lithos.2011.01.016](https://doi.org/10.1016/j.lithos.2011.01.016)
- Guo, G., Mao, W.L., Zhang, R.Y., Liou, J.G., Ernst, W., Yang, J., Liu, X., Xu, X., Zhang, Y., and Wu, B., 2021, Characteristics and implications of podiform-chromite hosted silicate inclusions in the Zedang ophiolite, Southern Tibet: *Lithos*, v. 396, p. 106218. [10.1016/j.lithos.2021.106218](https://doi.org/10.1016/j.lithos.2021.106218)
- Hall, R., and Sevastjanova, I., 2012, Australian crust in Indonesia: *Australian Journal of Earth Sciences*, v. 59, no. 6, p. 827–844. [10.1080/08120099.2012.692335](https://doi.org/10.1080/08120099.2012.692335)
- Hall, R., and Wilson, M., 2000, Neogene sutures in eastern Indonesia: *Journal of Asian Earth Sciences*, v. 18, no. 6, p. 781–808. [10.1016/S1367-9120\(00\)00040-7](https://doi.org/10.1016/S1367-9120(00)00040-7)
- Hasria, M., Asfar, S., Arisona, O., Restele, A., Ngkoimani, L.O., and Yustika, R., 2021, Characteristics of chromite deposits at North Kabaena District, Bombana Regency, Southeast Sulawesi Province, Indonesia: *Journal of Geoscience, Engineering, Environment, and Technology*, v. 6, no. 2, p. 94–98. [10.25299/jgeet.2021.6.2.6424](https://doi.org/10.25299/jgeet.2021.6.2.6424)
- Hu, W.-J., Zhou, M.-F., Yudovskaya, M.A., Vikentyev, I.V., Malpas, J., and Zhang, P.-F., 2022, Trace elements in chromite as indicators of the origin of the giant podiform chromite deposit at Kempirsai, Kazakhstan: *Economic Geology*, Vol. 117, p. 1629–1655
- Idrus, A., Septiana, S., Zaccarini, F., Garuti, G., and Hasria, H., 2022, Mineralogical, textural and chemical characteristics of ophiolitic chromite and platinum group minerals from Kabaena Island (Indonesia: Their Petrogenetic Nature and Geodynamic Setting: *Minerals*, v. 12, no. 5, p. 516.
- Irvine, T., 1965, Chromian spinel as a petrogenetic indicator: Part 1: Theory: *Canadian Journal of Earth Sciences*, v. 2, no. 6, p. 648–672.
- Irvine, T., 1967, Chromian spinel as a petrogenetic indicator: Part 2: Petrologic Applications: *Canadian Journal of Earth Sciences*, v. 4, no. 1, p. 71–103.
- Kadarusman, A., Miyashita, S., Maruyama, S., Parkinson, C.D., and Ishikawa, A., 2004, Petrology, geochemistry and paleogeographic reconstruction of the East Sulawesi Ophiolite, Indonesia: *Tectonophysics*, v. 392, no. 1–4, p. 55–83. [10.1016/j.tecto.2004.04.008](https://doi.org/10.1016/j.tecto.2004.04.008)
- Kamenetsky, V.S., Crawford, A.J., and Meffre, S., 2001, Factors controlling chemistry of magmatic spinel: An empirical

- study of associated olivine, Cr-spinel and melt inclusions from primitive rocks: *Journal of Petrology*, v. 42, no. 4, p. 655–671. [10.1093/petrology/42.4.655](https://doi.org/10.1093/petrology/42.4.655)
- Katili, J.A., 1978, Past and present geotectonic position of Sulawesi, Indonesia: *Tectonophysics*, v. 45, no. 4, p. 289–322. [10.1016/0040-1951\(78\)90166-X](https://doi.org/10.1016/0040-1951(78)90166-X)
- Khedr, M.Z., and Arai, S., 2012, Petrology and geochemistry of prograde deserpentinized peridotites from Happo-O'ne, Japan: Evidence of element mobility during deserpentinization: *Journal of Asian Earth Sciences*, v. 43, no. 1, p. 150–163. [10.1016/j.jseas.2011.08.017](https://doi.org/10.1016/j.jseas.2011.08.017)
- Khedr, M.Z., and Arai, S., 2017, Peridotite-chromitite complexes in the Eastern Desert of Egypt: Insight into neoproterozoic sub-arc mantle processes: *Gondwana Research*, v. 52, p. 59–79. [10.1016/j.gr.2017.09.001](https://doi.org/10.1016/j.gr.2017.09.001)
- Lago, B.L., Rabinowicz, M., and Nicolas, A., 1982, Podiform chromite ore bodies: A genetic model: *Journal of Petrology*, v. 23, no. 1, p. 103–125. [10.1093/petrology/23.1.103](https://doi.org/10.1093/petrology/23.1.103)
- Li, C., Naldrett, A.J., and Ripley, E.M., 2007, Controls on the Fe and Ni contents of olivine in sulfide-bearing mafic/ultramafic intrusions: Principles, modeling, and examples from Voisey's Bay: *Earth Science Frontiers*, v. 14, no. 5, p. 177–183. [10.1016/S1872-5791\(07\)60043-8](https://doi.org/10.1016/S1872-5791(07)60043-8)
- Liu, Y., Hu, Z., Gao, S., Günther, D., Xu, J., Gao, C., and Chen, H., 2008, In situ analysis of major and trace elements of anhydrous minerals by LA-ICP-MS without applying an internal standard: *Chemical Geology*, v. 257, no. 1–2, p. 34–43. [10.1016/j.chemgeo.2008.08.004](https://doi.org/10.1016/j.chemgeo.2008.08.004)
- Liu, X., and O'Neill, H.S.C., 2004, Partial melting of spinel lherzolite in the system CaO–MgO–Al₂O₃–SiO₂±K₂O at 1.1 GPa: *Journal of Petrology*, v. 45, no. 7, p. 1339–1368. [10.1093/petrology/egh021](https://doi.org/10.1093/petrology/egh021)
- Maurel, C., 1984, Étude expérimentale de l'équilibre spinelle chromifère–liquide silicaté basique: SFMC Meet. "Les spinelles", Lille, oral. comm.
- Melcher, F., Grum, W., Simon, G., Thalhammer, T.V., and Stumpfl, E.F., 1997, Petrogenesis of the ophiolitic giant chromite deposits of Kempirsai, Kazakhstan: A study of solid and fluid inclusions in chromite: *Journal of Petrology*, v. 38, no. 10, p. 1419–1458. [10.1093/etroj/38.10.1419](https://doi.org/10.1093/etroj/38.10.1419)
- Monnier, C., Girardeau, J., Maury, R.C., and Cotten, J., 1995, Back-arc basin origin for the East Sulawesi ophiolite (eastern Indonesia): *Geology*, v. 23, no. 9, p. 851–854. [10.1130/0091-7613\(1995\)023<0851:BABOFT>2.3.CO;2](https://doi.org/10.1130/0091-7613(1995)023<0851:BABOFT>2.3.CO;2)
- Mubroto, B., Briden, J., McClelland, E., and Hall, R., 1994, Palaeomagnetism of the Balantak ophiolite, Sulawesi: *Earth and Planetary Science Letters*, v. 125, no. 1–4, p. 193–209. [10.1016/0012-821X\(94\)90215-1](https://doi.org/10.1016/0012-821X(94)90215-1)
- Nayak, R., Pal, D., and Chinnasamy, S.S., 2021, High-Cr chromitites of the Nidar Ophiolite Complex, northern India: Petrogenesis and tectonic implications: *Ore Geology Reviews*, v. 129, p. 103942. [10.1016/j.oregeorev.2020.103942](https://doi.org/10.1016/j.oregeorev.2020.103942)
- Nursahan, I., 2005, Inventarisasi dan Evaluasi Mineral Logam di Daerah Kabupaten Bengkayang dan Kabupaten Landak, Provinsi Kalimantan Barat: Subdit Logam: Direktorat Inventarisasi Sumber Daya Mineral
- Pagé, P., and Barnes, S.-J., 2009, Using trace elements in chromites to constrain the origin of podiform chromitites in the Thetford Mines ophiolite, Québec, Canada: *Economic Geology*, v. 104, no. 7, p. 997–1018. [10.2113/econgeo.104.7.997](https://doi.org/10.2113/econgeo.104.7.997)
- Pan, -Q.-Q., Xiao, Y., Su, B.-X., Liu, X., Robinson, P.T., Cui, -M.-M., Wang, J., and Uysal, I., 2022, Fingerprinting stealth metasomatism in ophiolitic peridotites: *Lithos*, v. 424–425, p. 106755. [10.1016/j.lithos.2022.106755](https://doi.org/10.1016/j.lithos.2022.106755)
- Parkinson, C.D., 1996, The origin and significance of metamorphosed tectonic blocks in mélanges: Evidence from Sulawesi, Indonesia: *Terra Nova*, v. 8, no. 4, p. 312–323. [10.1111/j.1365-3121.1996.tb00564.x](https://doi.org/10.1111/j.1365-3121.1996.tb00564.x)
- Parkinson, C., 1998, Emplacement of the East Sulawesi Ophiolite: Evidence from subophiolite metamorphic rocks: *Journal of Asian Earth Sciences*, v. 16, no. 1, p. 13–28. [10.1016/S0743-9547\(97\)00039-1](https://doi.org/10.1016/S0743-9547(97)00039-1)
- Pearce, J.A., van der Laan, S.R., Arculus, R.J., Murton, B.J., Ishii, T., Peate, D.W., and Parkinson, I.J., 1992, Boninite and harzburgite from Leg 125 (Bonin-Mariana forearc): A case study of magma genesis during the initial stages of subduction: *Proceedings of the ocean drilling program, Scientific Results*, v. 125, p. 623–659.
- Perkins, D., and Anthony, E.Y., 2011, The evolution of spinel lherzolite xenoliths and the nature of the mantle at Kilbourne Hole, New Mexico: *Contributions to Mineralogy and Petrology*, v. 162, no. 6, p. 1139–1157. [10.1007/s00410-011-0644-1](https://doi.org/10.1007/s00410-011-0644-1)
- Plechov, P.Y., Shcherbakov, V., and Nekrylov, N., 2018, Extremely magnesian olivine in igneous rocks: *Russian Geology and Geophysics*, v. 59, no. 12, p. 1702–1717. [10.1016/j.rgg.2018.12.012](https://doi.org/10.1016/j.rgg.2018.12.012)
- Pujol-Solà, N., Domínguez-Carretero, D., Proenza, J.A., Haissen, F., Ikenne, M., González-Jiménez, J.M., Colás, V., Maacha, L., and Garcia-Casco, A., 2021, The chromitites of the neoproterozoic Bou Azzer ophiolite (central Anti-Atlas, Morocco) revisited: *Ore Geology Reviews*, v. 134, p. 104166. [10.1016/j.oregeorev.2021.104166](https://doi.org/10.1016/j.oregeorev.2021.104166)
- Pujol-Solà, N., Garcia Casco, A., Proenza, J., González-Jiménez, J., Del Campo, A., Colás, V., Sánchez Navas, A., and Roqué-Rosel, J., 2020, Diamond forms during low pressure serpentinisation of oceanic lithosphere.
- Pujol-Solà, N., Proenza, J.A., Garcia-Casco, A., González-Jiménez, J.M., Andreazini, A., Melgarejo, J.C., and Gervilla, F., 2018, An alternative scenario on the origin of ultra-high pressure (UHP) and super-reduced (SUR) minerals in ophiolitic chromitites: A case study from the mercedita deposit (Eastern Cuba: *Minerals*, v. 8, no. 10, p. 433. [10.3390/min8100433](https://doi.org/10.3390/min8100433)
- Putirka, K.D., 2008, Thermometers and barometers for volcanic systems: *Reviews in Mineralogy and Geochemistry*, v. 69, no. 1, p. 61–120. [10.2138/rmg.2008.69.3](https://doi.org/10.2138/rmg.2008.69.3)
- Robinson, P.T., Bai, W.-J., Malpas, J., Yang, J.-S., Zhou, M.-F., Fang, Q.-S., Hu, X.-F., Cameron, S., and Staudigel, H., 2004, Ultra-high pressure minerals in the Luobusa Ophiolite, Tibet, and their tectonic implications: *Geological Society, London, Special Publications*, v. 226, no. 1, p. 247–271. [10.1144/GSL.SP.2004.226.01.14](https://doi.org/10.1144/GSL.SP.2004.226.01.14)
- Roeder, P., Gofton, E., and Thornber, C., 2006, Cotectic proportions of olivine and spinel in olivine-tholeiitic basalt and evaluation of pre-eruptive processes: *Journal of Petrology*, v. 47, no. 5, p. 883–900. [10.1093/petrology/egi099](https://doi.org/10.1093/petrology/egi099)
- Rollinson, H., 2008, The geochemistry of mantle chromitites from the northern part of the Oman ophiolite: Inferred parental melt compositions: *Contributions to Mineralogy and Petrology*, v. 156, no. 3, p. 273–288. [10.1007/s00410-008-0284-2](https://doi.org/10.1007/s00410-008-0284-2)

- Sepidbar, F., Khedr, M.Z., Ghorbani, M.R., Palin, R.M., and Xiao, Y., 2021, Petrogenesis of arc-related peridotite hosted chromitite deposits in Sikhoran-Soghan mantle section, South Iran: Evidence for proto-forearc spreading to boninitic stages: *Ore Geology Reviews*, v. 136, p. 104256. [10.1016/j.oregeorev.2021.104256](https://doi.org/10.1016/j.oregeorev.2021.104256)
- Septiana, S., Idrus, A., Zaccarini, F., Garuti, G., and Setijadji, L., 2021, Ore mineralogy of podiform-type chromite deposit in Tedubara area and its vicinity, Kabaena Island, Indonesia, in *Proceedings IOP Conference Series: Earth and Environmental Science*, NIT Raipur, India, v. 851, no. 1, IOP Publishing, p. 12044.
- Sideridis, A., Zaccarini, F., Koutsovitis, P., Grammatikopoulos, T., Tsikouras, B., Garuti, G., and Hatzipanagioutou, K., 2021, Chromitites from the Vavdos ophiolite (Chalkidiki, Greece): Petrogenesis and geotectonic settings; constrains from spinel, olivine composition, PGE mineralogy and geochemistry: *Ore Geology Reviews*, v. 137, p. 104289. [10.1016/j.oregeorev.2021.104289](https://doi.org/10.1016/j.oregeorev.2021.104289)
- Silver, E.A., McCaffrey, R., Joyodiwiryono, Y., and Stevens, S., 1983, Ophiolite emplacement by collision between the Sula Platform and the Sulawesi island arc: Indonesia: *Journal of Geophysical Research: Solid Earth*, v. 88, no. B11, p. 9419–9435. [10.1029/JB088iB11p09419](https://doi.org/10.1029/JB088iB11p09419)
- Simandjuntak, T., 1992, New data on the age of ophiolite in eastern Sulawesi.
- Simandjuntak, T., Situmorang, R., and Hadiwijoyo, S., 1987, Geologic map of the Batui Quadrangle, Sulawesi. 1: 250,000: Bandung, Indonesia, Geological Research & Development Centre.
- Simandjuntak, T., Surono, and Sukido, 1993, Peta Geologi Lembar Kolaka, Sulawesi, Skala 1:250.000: Bandung, Pusat Penelitian dan Pengembangan Geologi.
- Sobolev, A.V., Hofmann, A.W., Kuzmin, D.V., Yaxley, G.M., Arndt, N.T., Chung, S.-L., Danyushevsky, L.V., Elliott, T., Frey, F.A., and Garcia, M.O., 2007, The amount of recycled crust in sources of mantle-derived melts: *Science*, v. 316, no. 5823, p. 412–417. [10.1126/science.1138113](https://doi.org/10.1126/science.1138113)
- Spandler, C., O'Neill, H.S.C., and Kamenetsky, V.S., 2007, Survival times of anomalous melt inclusions from element diffusion in olivine and chromite: *Nature*, v. 447, no. 7142, p. 303–306. [10.1038/nature05759](https://doi.org/10.1038/nature05759)
- Stowe, C.W., 1987, Evolution of chromium ore fields, New York: Van Nostrand Reinhold, p. 340
- Su, B.-X., Robinson, P.T., Chen, C., Xiao, Y., Melcher, F., Bai, Y., Gu, X.-Y., Uysal, I., and Lenaz, D., 2020, The occurrence, origin, and fate of water in chromitites in ophiolites: *American Mineralogist*, v. 105, no. 6, p. 894–903. [10.2138/am-2020-7270](https://doi.org/10.2138/am-2020-7270)
- Su, B., Zhou, M., Jing, J., Robinson, P.T., Chen, C., Xiao, Y., Liu, X., Shi, R., Lenaz, D., and Hu, Y., 2019, Distinctive melt activity and chromite mineralization in Luobusa and Purang ophiolites, southern Tibet: Constraints from trace element compositions of chromite and olivine: *Science Bulletin*, v. 64, no. 2, p. 108–121. [10.1016/j.scib.2018.12.018](https://doi.org/10.1016/j.scib.2018.12.018)
- Tamura, A., and Arai, S., 2006, Harzburgite–dunite–orthopyroxene suite as a record of supra-subduction zone setting for the Oman ophiolite mantle: *Lithos*, v. 90, no. 1–2, p. 43–56. [10.1016/j.lithos.2005.12.012](https://doi.org/10.1016/j.lithos.2005.12.012)
- Uysal, I., Tarkian, M., Sadiklar, M.B., Zaccarini, F., Meisel, T., Garuti, G., and Heidrich, S., 2009, Petrology of Al- and Cr-rich ophiolitic chromitites from the Muğla, SW Turkey: Implications from composition of chromite, solid inclusions of platinum-group mineral, silicate, and base-metal mineral, and Os-isotope geochemistry: *Contributions to Mineralogy and Petrology*, v. 158, no. 5, p. 659–674. [10.1007/s00410-009-0402-9](https://doi.org/10.1007/s00410-009-0402-9)
- Walker, D., and Cameron, W., 1983, Boninite primary magmas: Evidence from the Cape Vogel Peninsula, PNG: *Contributions to Mineralogy and Petrology*, v. 83, no. 1, p. 150–158. [10.1007/BF00373088](https://doi.org/10.1007/BF00373088)
- Wang, X.B., and Bao, P.S., 1987, The genesis of podiform chromite deposits—A case study of the Luobusa chromite deposit, Tibet: *Chinese Journal of Geology*, v. 22, p. 166–181.
- Xiao, Y., Teng, F.Z., Su, B.X., Hu, Y., Zhou, M.F., Zhu, B., Shi, R.D., Huang, Q.S., Gong, X.H., and He, Y.S., 2016, Iron and magnesium isotopic constraints on the origin of chemical heterogeneity in podiform chromitite from the Luobusa ophiolite, Tibet: *Geochemistry: Geophysics, Geosystems*, v. 17, no. 3, p. 940–953. [10.1002/2015GC006223](https://doi.org/10.1002/2015GC006223)
- Xiong, F., Yang, J., Robinson, P.T., Xu, X., Liu, Z., Li, Y., Li, J., and Chen, S., 2015, Origin of podiform chromitite, a new model based on the Luobusa ophiolite, Tibet: *Gondwana Research*, v. 27, no. 2, p. 525–542. [10.1016/j.jgr.2014.04.008](https://doi.org/10.1016/j.jgr.2014.04.008)
- Yamamoto, S., Komiya, T., Hirose, K., and Maruyama, S., 2009, Coesite and clinopyroxene exsolution lamellae in chromites: In-situ ultrahigh-pressure evidence from podiform chromitites in the Luobusa ophiolite, southern Tibet: *Lithos*, v. 109, no. 3–4, p. 314–322. [10.1016/j.lithos.2008.05.003](https://doi.org/10.1016/j.lithos.2008.05.003)
- Yang, J., Meng, F., Xu, X., Robinson, P.T., Dilek, Y., Makeyev, A.B., Wirth, R., Wiedenbeck, M., and Cliff, J., 2015, Diamonds, native elements and metal alloys from chromitites of the Ray-Iz ophiolite of the Polar Urals: *Gondwana Research*, v. 27, no. 2, p. 459–485. [10.1016/j.jgr.2014.07.004](https://doi.org/10.1016/j.jgr.2014.07.004)
- Yao, J., Zhang, G., Wang, S., and Zhao, J., 2021b, Recycling of carbon from the stagnant paleo-Pacific slab beneath Eastern China revealed by olivine geochemistry: *Lithos*, v. 398–399, p. 106249. [10.1016/j.lithos.2021.106249](https://doi.org/10.1016/j.lithos.2021.106249)
- Yao, J.-H., Zhu, W.-G., Li, C., Zhong, H., Bai, Z.-J., Ripley, E.M., and Li, C., 2018, Petrogenesis and ore genesis of the Lengshuiqing magmatic sulfide deposit in southwest China: Constraints from chalcophile elements (PGE, Se) and Sr-Nd-Os-S isotopes: *Economic Geology*, v. 113, no. 3, p. 675–698. [10.5382/econgeo.2018.4566](https://doi.org/10.5382/econgeo.2018.4566)
- Yao, J.-H., Zhu, W.-G., Li, C., Zhong, H., Yu, S., Ripley, E.M., and Bai, Z.-J., 2019, Olivine O isotope and trace element constraints on source variation of picrites in the Emeishan flood basalt province, SW China: *Lithos*, Vol. 338, p. 87–98
- Yao, J.-H., Zhu, W.-G., Wang, Y.-J., Zhong, H., and Bai, Z.-J., 2021a, Geochemistry of the Yumen picrites-basalts from the Emeishan large igneous province: Implications for their mantle source, PGE behaviors, and petrogenesis: *Lithos*, v. 400, p. 106364. [10.1016/j.lithos.2021.106364](https://doi.org/10.1016/j.lithos.2021.106364)
- Zaccarini, F., Garuti, G., Proenza, J.A., Campos, L., Thalhammer, O.A., Aiglsperger, T., and Lewis, J.F., 2011, Chromite and platinum group elements mineralization in the Santa Elena Ultramafic Nappe (Costa Rica): Geodynamic implications: *Geologica Acta: an International Earth Science Journal*, v. 9, no. 3–4, p. 407–423.
- Zaccarini, F., Idrus, A., and Garuti, G., 2016, Chromite composition and accessory minerals in chromitites from Sulawesi,

- Indonesia: Their genetic significance: *Minerals*, v. 6, no. 2, p. 46. [10.3390/min6020046](https://doi.org/10.3390/min6020046)
- Zhang, Y., Jin, Z., Griffin, W.L., Wang, C., and Wu, Y., 2017, High-pressure experiments provide insights into the Mantle Transition Zone history of chromitite in Tibetan ophiolites: *Earth and Planetary Science Letters*, v. 463, p. 151–158. [10.1016/j.epsl.2017.01.036](https://doi.org/10.1016/j.epsl.2017.01.036)
- Zhou, M.-F., Robinson, P., and Bai, W., 1994, Formation of podiform chromitites by melt/rock interaction in the upper mantle: *Mineralium Deposita*, v. 29, no. 1, p. 98–101. [10.1007/BF03326400](https://doi.org/10.1007/BF03326400)
- Zhou, M.-F., Robinson, P., Malpas, J., Aitchison, J., Sun, M., Bai, W.-J., Hu, X.-F., and Yang, J.-S., 2001, Melt/mantle interaction and melt evolution in the Sartohay high-Al chromite deposits of the Dalabute ophiolite (NW China): *Journal of Asian Earth Sciences*, v. 19, no. 4, p. 517–534. [10.1016/S1367-9120\(00\)00048-1](https://doi.org/10.1016/S1367-9120(00)00048-1)
- Zhou, M.-F., Robinson, P.T., Su, B.-X., Gao, J.-F., Li, J.-W., Yang, J.-S., and Malpas, J., 2014, Compositions of chromite: Associated Minerals, and Parental Magmas of Podiform Chromite Deposits: the Role of Slab Contamination of Asthenospheric Melts in Suprasubduction Zone Environments: *Gondwana Research*, v. 26, p. 262–283
- Zhou, M.-F., Sun, M., Keays, R.R., and Kerrich, R.W., 1998, Controls on platinum-group elemental distributions of podiform chromitites: A case study of high-Cr and high-Al chromitites from Chinese orogenic belts: *Geochimica et Cosmochimica Acta*, v. 62, no. 4, p. 677–688. [10.1016/S0016-7037\(97\)00382-7](https://doi.org/10.1016/S0016-7037(97)00382-7)